

Ameliorative Effects of Dates on induced Toxicity of Aflatoxin B1 on the Renal Cortex of Adult Male Albino Rats: Histological, Immunohistochemical and biochemical Study

Original
Article

Maha El-Sayed Soliman¹, Reem Mohamed Ghareb El-Sharkawy², Mona Mohamed Hassan Soliman³, Ghada Hasan Elsaify⁴, Rania Ibrahim yassein⁵

^{1,2,4,5}Departments of Histology and Cell Biology, Faculty of Medicine, Menoufia University,
³Department of Microbiology and Immunology, Veterinary Division, National Research Centre, Doki, Egypt.

ABSTRACT

Introduction: Aflatoxin B1 is a highly toxic mycotoxin. Dates are considered curative plants which are highly effective antidotes.

Aim: This study is to investigate the induced histological & histochemical effects of AFB1 on the renal cortex of adult male albino rats & the possible ameliorative role of dates.

Materials and Methods: Sixty male adult albino rats were utilized. They were divided into four main groups: control group (group I) (n=20), dates treated group (group II) (n=10), Aflatoxin B1 treated group (group III) (n=20), we sacrificed half of them after 2 weeks (subgroup IIIa) and the other half left without any treatment for another 2 weeks as a recovery subgroup (subgroup IIIb), and Aflatoxin and dates treated group (group IV) (n=10). At the end of study, animals were anesthetized for taking the blood samples for kidney function then kidneys were dissected out and processed it for histological and immunohistochemical study.

Results: H&E stained sections of subgroup IIIa showed various degenerative changes of renal cortex, together with increased collagen deposition as denoted by Mallory stain. There was intense PAS reaction in Bowman's capsule and basement membrane of renal tubules. Electron microscopic results were matched with light microscopic results. Immunohistochemical revealed intensive PAX2 in podocytes. Recovery subgroup revealed partial enhancement. Examination of group IV showed that renal cortex nearly normal architecture.

Conclusion: AFB1 has severe damaging effects on renal cortex. These effects were partially improved after cessation of treatment. But these effects are extremely attenuated with dates.

Key Words: Aflatoxin B1, Dates, kidney, PAX2.

Revised: 20 July 2020, **Accepted:** 28 August 2020.

Corresponding Author: Reem Mohamed Ghareb El-Sharkawy, MSc, Departments of Histology and Cell Biology, Faculty of Medicine, Menoufia University, Egypt. **Tel.:** 01200879981, **E-mail:** reem_mohamed49@yahoo.com

ISSN:2536-9172, December 2020, Vol. 4, No. 2

INTRODUCTION

Many researches have been done on Aflatoxins studying their toxic effects on various organs. Four types of Aflatoxins were detected; Aflatoxins B1, B2, G1, and G2 Aflatoxin B1 (AFB1) is the highly toxic & most common type of Aflatoxins^[1].

Both *Aspergillus flavus* and *Aspergillus parasiticus* produce AFB1^[2]. It resists heating^[3]. Corn and peanuts are main sources of Aflatoxins^[4].

AB1 is found to be hepatotoxic, nephrotoxic, mutagenic, genotoxic, carcinogenic, and immune-suppressive agent in human and animals^[5].

Oxidative stress plays an important role in AFB1 toxicity that proved by decreased antioxidant parameters associated with apoptosis^[6].

Recently in the last decades, there is an increased trend for the use of natural medicaments instead of traditional treatments for the treatment of many diseases^[7].

Dates are rich in sugar, but have low protein and fat contents. It contains antioxidant flavenoids^[8]. Dates have an important role in the absorption and neutralization of free radicals due to its high concentration of polyphenols which have antioxidant activity^[9].

We performed this study to evaluate the induced histological and histochemical toxic effects of Aflatoxin B1 on the renal cortical tissues of adult male albino rats & to compare between aflatoxin and dates group and the recovery subgroup.

MATERIALS AND METHODS

Animals

Sixty (60) adult male albino rats 3 months old were used weighing nearly 140-170 gm in the present study. They were housed in stainless metal cages at room temperature. Laboratory rat chow diet and water ad-libitum were available. The general conditions and behavior of the animals were noticed. Strict care and hygiene were provided to maintain a normal and healthy environment for the rats all time of the experiment. This experiment was carried out in the Animal House of Faculty of Medicine, Menoufia University.

Chemicals

1- Aflatoxin B1: It was obtained from Microbiology and Immunology Department of The National Research Center in Dokki, Cairo. It was in the form of powder, which is yellowish white in color. (1mg) Aflatoxin was dissolved in (143) ml olive oil to produce the desire concentration (7µg /1ml) and a dose of 1.2 ml/rat was taken orally by sterile plastic syringe as method done by Al-Ghasham *et al.*^[10].

2- Standards of Aflatoxin: B1, B2, G1 and G2, methanol, trifluoroacetic acid, acetonitrile, acetic acid, mercaptoethanol and disodium tetra borate were purchased from Sigma Chemical Co (St. Louis, MO, U.S.A.). All the used solvents and chemicals were of high performance liquid chromatography (HPLC) grade.

3- Aqueous extract of Dates: Dates were purchased from market and dissolved in distilled water (1 kilogram of dates and 1 liter of distilled water were stirred in the mixer to be easily taken by the rats) to produce the desire concentration 1mg/1ml and a dose of 1.7 ml/rat was taken orally by sterile plastic syringe as method done by Al-Ghasham *et al.*^[10].

Groups

60 male adult albino rats were used and divided randomly into four main groups. They all received treatment by oral route, by sterile plastic syringe for 2 weeks. All groups were sacrificed after 2 weeks from the start of the experiment except group IIIb animals were left for 4 weeks:-

1-Group I (control group):

It included 20 animals which then were subdivided into 2 equal subgroups:

- **subgroup Ia** composed of 10 animals received distilled water (the dissolvent of dates)
- **subgroup Ib** composed of 10 animals received olive oil (the dissolvent of Aflatoxin).

2-Group II (Dates group):

It included 10 animals that received aqueous date extract at a dose of (10 mg/kg)^[10].

3-Group III (Aflatoxin B1 group):

It included 20 animals which received AFB1 at a dose 50 µg/kg^[10]. Then it was subdivided into 2 equal subgroups, subgroup IIIa included half of the animals which were sacrificed after 2 weeks, we left the other half without treatment for another 2 weeks then they were sacrificed and considered as subgroup IIIb. These 10 animals will be left for 4 weeks as a recovery subgroup without treatment

4-Group IV (Aflatoxin B1 and dates group):

It included 10 animals. They received Aflatoxin B1 and dates concomitantly with the same dose and period.

Methods

1- Biochemical study

At the end of the experiment, blood samples were obtained from the vein of the tip of tail of all rats and analyzed for serum levels of urea and creatinine by using an auto analyzer (Hitachi 912 Auto-Analyzer; Hitachi, Germany)^[11].

2- Histological study

A -Light microscopic examination:

The animals from all groups were anaesthetized by ether at the end of the experiment. The two kidneys of each rat were carefully dissected out, one kidney was fixed in 10% formal saline for the following stains Hematoxylin and Eosin (H&E)^[12], Toluidine blue^[13], Mallory Trichrome Technique (M.T)^[14] and Periodic Acid-Schiff's Reaction (PAS)^[12].

B-Electron microscopic examination:

The other kidney was processed for electron microscopic study, cut into small pieces and rapidly fixed in 3% glutaraldehyde and 0.1 M phosphate buffer at pH 7.4. The blocks were trimmed and cut into semi thin and ultrathin sections. The ultrathin sections of about 50-80 nm thickness obtained by using diamond knife. The sections were mounted on copper grids, stained by uranyl acetate in 50% ethanol then Reynolds lead citrate and then examined by Transmission Electron Microscope (Tanta EM Centre, Tanta Faculty of Medicine)^[13].

3- Immunohistochemical study:

Paired Box Gene 2 (PAX2) was used for detection of glomerular injury. According to Li Li *et al.*^[15], ready to use primary rabbit anti-human PAX2 monoclonal antibody

diluted form (MAD-00065OQD-7) was applied and incubated according to manufacturer's protocol (Thermo Fisher Scientific Anatomical Pathology) with catalog number TP-060-HL, it was washed 4 times in buffer, then Biotinylated Goat Anti-Polyvalent was applied and incubated for 10 minutes at room temperature and finally washed 4 times in buffer. Streptavidin Peroxidase was applied and incubated for 10 minutes at room temperature. Then rinsed 4 times in buffer. Then incubated with peroxidase compatible chromogen according to manufacturer's recommendations. Then counterstained with hematoxylin and coverslip. The specificity and sensitivity of antigen detection is dependent on the specific primary antibody used. The nuclei stained brown. Negative control was done by additional specimens of kidney that processed in the same way but omitting treatment with the primary antibody whereas the ovary was the positive control.

4- Statistical analysis

All parameters for all animals – body weight, kidney weight and serum levels of urea and creatinine were measured. The collected data were tabulated and analyzed using statistical package for the Social Science Software (SPSS) (version 17.0 on an IBM compatible computer; SPSS Inc., Chicago, Illinois, USA). Statistically significant difference was determined by one-way analysis of variance (ANOVA), followed by the least significant difference test for comparison among groups and using Student's t-tests for two-group comparisons. Non-significant if $P > 0.05$, significant if $P < 0.05$ and highly significant if $P < 0.001$ ^[6].

5- Determination of Aflatoxins concentration using high performance liquid chromatography with fluorescence detection (HPLC-FLD)

HPLC-FLD apparatus:

High performance liquid chromatography (HPLC) assay was performed utilizing Agilent Technologies 1100 series liquid chromatograph along with an auto sampler and Fluorescence detector. The analytical column was an Eclipse XDB-C18 (150 X 4.6 μm ; 5 μm) with a C18 guard column (Agilent, USA).

I. Derivatization:

The derivatization process was performed as described in^[7]. Mixture of 9 acetonitrile: 1 methanol was used to dissolved standard solutions of Aflatoxins.

II- HPLC conditions:

The components of mobile phase were Acetonitrile/Water/Methanol (1:6:3). Isocratic separation was implemented at room temperature with 1.0 ml/min flow rate and 20 μl from both the standard solutions and the chloroform extracts were injected. The used detector was of fluorescence type at wavelength of 365 nm for excision

and 450 nm for emission. A 0.45 μm Acrodisc syringe filter (Gelman Laboratory, MI) was utilized to filtrate the samples before injection. Matching and analyzing retention times of both standards and samples was done^[18].

RESULTS

The general condition:

Abnormal behavior of animals was observed, they appeared lazy. After 2 days from starting our study one animal died from the aflatoxin subgroup. After one week one animal died from the control group. In the 12th day another 2 animals died from the aflatoxin subgroup. After 4 weeks one animal died from the recovery subgroup.

Kidneys of the aflatoxin subgroup and recovery subgroup were swollen and showed hemorrhage while kidneys of aflatoxin and dates group showed no hemorrhage and were nearly similar to control.

Histological study

Light microscopic examination

1) H&E stain:

Group I & II (control and dates)

Sections of renal cortex of control and dates groups were almost similar showing normal structure of renal cortex. It was formed of glomeruli surrounded by proximal and distal convoluted tubules. The glomerulus was surrounded by capsule had parietal layer lined by simple squamous epithelium and visceral layer lined by podocytes with distinct capsular space in between. Proximal convoluted tubules with narrow lumen were lined by pyramidal cells. Distal convoluted tubules with wide lumen were lined by simple cubical cells. (Figs. 1A, 1B, 2A & 2B).

Subgroup IIIa (Aflatoxin B1)

Sections of renal cortex of Aflatoxin B1 subgroup revealed severe focal affection of structure of the renal cortex. They showed apparently enlarged glomerulus with segmentation of its tufts of Capillaries and apparently increased capsular space (Fig. 1C1). Other degenerated glomeruli with intraglomerular congestion were seen (Figs. 1C2 & 2C2). The proximal and distal tubules showed degeneration of the cells in the form of darkly stained nuclei (Figs. 1C2, 2C1 & 2C2). Tubules appeared vacuolated (Fig. 1C1 & 2C1). Some tubules showed tubular necrosis with intratubular epithelial debris (Fig.1C1). Massive loss of renal tubules was also demonstrated (Fig.1C1). Blood vessels showed dilatation and congestion (Fig. 2C2). The interstitium between tubules was infiltrated by inflammatory cells (Figs. 1C1 & 1C2). Interstitial hemorrhage was also observed (Figs. 1C2 & 2C2).

Subgroup IIIb (Recovery)

Sections of renal cortex of recovery subgroup showed minimal improvement. Most of renal corpuscles were still affected, the glomerulus showed some degenerations with partial damaged renal capsule. The renal tubules were moderately improved when compared with the AFB1 treated group. The proximal and distal convoluted tubules showed that disorganization and vacuolations were still seen. They were lined by darkly stained nuclei. Some tubules showed apparent tubular necrosis with intratubular epithelial debris and cellular infiltration beside the glomerulus (Fig. 1D & 2D).

Group IV (Aflatoxin and dates)

Sections of renal cortex of Aflatoxin and dates group showed partial improvement. Apparently normal renal corpuscles were surrounded by partially detached renal tubules nearly similar to that of control. The renal tubules were mildly affected when compared with the AFB1 treated group. Vacuolations were not seen. Apparently less cellular infiltration than that of the aflatoxin subgroup was seen (Figs. 1E & 2E).

2) Toluidine blue stain:

Group I & II (control and dates)

Sections of renal cortex of control and dates groups revealed glomerulus with tuft of capillaries lined by endothelial cells, the spaces between the capillaries showed mesangial cells. The glomerulus was surrounded by parietal layer lined by flattened cells and visceral layer lined by podocytes. The proximal tubules were lined by pyramidal cells with central nuclei and apparent nucleoli and showed basal striations. The distal tubules were also lined by cubical cells with central nuclei and apparent nucleoli. There was minimal interstitial space in between the tubules (Figs. 3A & 3B).

Subgroup IIIa (Aflatoxin B1)

Sections of renal cortex of Aflatoxin B1 subgroup revealed glomerulus with dilated and congested capillaries, dilated capsular space and disorganized renal capsule lined by parietal layer with loss of the flattened cells and visceral layer with apparently enlarged podocytes. The proximal and distal tubules were lined by cells with darkly stained nuclei. The cells of proximal and distal tubules showed cytoplasmic vacuoles. Wide interstitial space between the tubules showed hemorrhage and cellular infiltration (Fig. 3C1 & 3C2).

Subgroup IIIb (Recovery)

Sections of renal cortex of recovery subgroup revealed glomerulus with capillaries with congestion and ruptured renal corpuscle lined by parietal layer with flattened nuclei and visceral layer with apparently enlarged podocytes. The cells of proximal and distal tubules were lined by

central vesicular nuclei. The cells of the tubules showed cytoplasmic vacuoles. Wide interstitial space between the tubules still showed cellular infiltration and hemorrhage. (Fig. 3D).

Group IV (Aflatoxin and dates)

Sections of renal cortex of Aflatoxin and dates group revealed glomerulus with capillaries with mild congestion, the glomerulus was surrounded by parietal layer with flattened nuclei and visceral layer with podocytes and minimal capsular space in between. The cells of proximal and distal tubules were lined by vesicular nuclei. The cells of tubules showed less cytoplasmic vacuoles than the aflatoxin subgroup. Wide interstitial space between the tubules was seen and there were apparently less cellular infiltration and hemorrhage than that of the aflatoxin subgroup (Fig. 3E).

Mallory trichrome stain:

Sections of renal cortex of control and dates groups revealed minimal amount of collagenous fibers around Bowman's capsule, proximal and distal tubules (Figs. 4A&4B). While sections of renal cortex of Aflatoxin B1 subgroup revealed massive amount of collagenous fibers around Bowman's capsule, proximal and distal tubules (Fig. 4C). Sections of renal cortex of recovery subgroup revealed moderate increase in collagenous fibers around Bowman's capsule, proximal and distal tubules in comparison with that of the aflatoxin subgroup but still more than that of control group (Fig. 4D). But sections of renal cortex of aflatoxin and dates group revealed mild amount of collagenous fibers around Bowman's capsule, proximal and distal tubules nearly similar to the control group (Fig. 4E).

Periodic Acid schiff's reaction (PAS):

Group I & II (control and dates)

Sections of renal cortex of control and dates group showed intense PAS reaction in both Bowman's capsule and basement membrane of renal tubules (Figs. 5A&5B).

Subgroup IIIa (Aflatoxin B1)

Sections of renal cortex of Aflatoxin B1 subgroup showed weak PAS reaction in both Bowman's capsule and basement membrane of renal tubules (Fig. 5C).

Subgroup IIIb (Recovery)

Sections of renal cortex of recovery subgroup showed mild PAS reaction in both Bowman's capsule and basement membrane of renal tubules (Fig. 5D).

Group IV (Aflatoxin and dates)

Sections of renal cortex of Aflatoxin and dates group showed moderate PAS reaction in both Bowman's capsule and basement membrane of renal tubules (Fig. 5E).

Electron microscopic examination

Group I & II (control and dates)

Sections of renal cortex of control and dates groups showed distinct capsular space (Fig. 6A), its visceral layer was lined by podocyte with euchromatic nucleus (Fig. 7A). Mesangial cell with euchromatic nucleus showed between capillaries (Fig. 8A). The blood renal barrier showed distinct glomerular basement membrane (GBM), non-fused podocyte foot processes and fenestrated endothelial cells on the other side (Figs. 9A&9B). Proximal convoluted tubules showed pyramidal cells with euchromatic nucleus and central nucleolus. Extensive basal infoldings with many elongated basal mitochondria were observed. Lysosomes in the form of electron dense bodies were also noticed in the cytoplasm. Long apical microvilli were noticed (Figs. 10A&10B). Distal convoluted tubules showed cubical cells with euchromatic nucleus and central nucleolus. Many basal infoldings with numerous elongated mitochondria in between were seen. No apical microvilli were noticed (Figs. 11A&11B).

Subgroup IIIa (Aflatoxin B1)

Sections of renal cortex of Aflatoxin B1 subgroup showed apparently dilated capsular space (Fig. 6C), its visceral layer was lined by irregular podocyte with ballooned vacuolated mitochondria and rarified cytoplasm (Fig. 7C). The space between capillaries showed irregular shaped mesangial cell with shrunken pyknotic nucleus (Fig. 8C). Neutrophilic infiltration with darkly stained nuclei was observed (Fig. 6C). Intraglomerular congestion was noticed (Figs. 7C&7E). Distorted structure of the blood renal barrier showed thickened glomerular basement membrane, distortion of the podocyte foot processes and fused endothelial cells on the other side (Figs. 9C1&9C2). Proximal convoluted tubules showed lining cells with irregular shrunken nuclei (10C1). Other nuclei had dilated prenuclear space (Fig. 10C2). Shedding of the cytoplasm in the lumen was seen (Fig. 10C1). There were many lysosomes and many cytoplasmic vacuolations (Figs. 10C2). Swollen mitochondria and closely packed apical microvilli were noticed (Figs. 10C1&10C2). Distal convoluted tubules showed euchromatic nucleus displaced more apically, loss of basal infoldings and abnormal distributed mitochondria. Fused cytoplasmic vacuoles were seen (Fig. 11C1), other multiple small cytoplasmic vacuoles and rarefaction of the cytoplasm were noticed (Figs. 11C1& 11C2). Cellular infiltration in the interstitium (Fig. 11C2) and interstitial hemorrhage were seen (Fig. 11C1).

Subgroup IIIb (Recovery)

Sections of renal cortex of recovery subgroup showed apparently improved blood renal barrier with apparently less thickening of the GBM, distortion of the podocyte foot processes and fused endothelial cells on the other side (Fig. 9D). Proximal convoluted tubules showed lining cells with euchromatic nuclei and abnormal shaped

mitochondria. Multiple lysosomes were seen. There were closely packed apical microvilli and shedded cytoplasm in the lumen (Fig. 10D). Distal convoluted tubules showed lining cells with irregular euchromatic indented nucleus and another nucleus with prenuclear space. Basally located swollen mitochondria and multiple cytoplasmic vacuoles were seen (Fig. 11D).

Group IV (Aflatoxin and dates)

Sections of renal cortex of Aflatoxin and dates group showed apparently less capsular space than the Aflatoxin treated group (Fig. 6E). Its visceral layer was lined by apparently enlarged podocyte with large irregular shaped nucleus and vacuolated cytoplasm (Fig. 7E). The space between capillaries showed apparently normal mesangial cell with euchromatic nucleus (Fig. 8E). Apparently less thickening of the GBM than that of the Aflatoxin group, non-fused podocyte foot processes and fenestrated endothelial cells on the other side were seen (Fig. 9E). Proximal convoluted tubules showed lining cells with euchromatic nucleus and swollen mitochondria. Long apical microvilli and shedded cytoplasm in the lumen were seen. (Fig. 10E). Distal convoluted tubules showed lining cells with apical euchromatic nucleus. Basal infoldings with apparently normal shaped mitochondria in between were detected. Vacuolations of the cytoplasm were seen (Fig. 11E).

Immunohistochemical study

Group I & II (control and dates)

Sections of renal cortex of control and dates groups showed intense expression of PAX2 in nuclei of distal tubules but negative expression in nuclei of podocytes (Figs. 12A&12B).

Subgroup IIIa (Aflatoxin B1)

Sections of renal cortex of Aflatoxin B1 subgroup showed intense expression of PAX2 in nuclei of both podocytes and distal tubules (Fig. 12C).

Subgroup IIIb (Recovery)

Sections of renal cortex of recovery subgroup showed moderate expression of PAX2 in nuclei of both podocytes and distal convoluted tubules (Fig. 12D)

Group IV (Aflatoxin and dates)

Sections of renal cortex of Aflatoxin and dates group showed mild expression of PAX2 in nuclei of both podocytes and distal convoluted tubules (Fig. 12E).

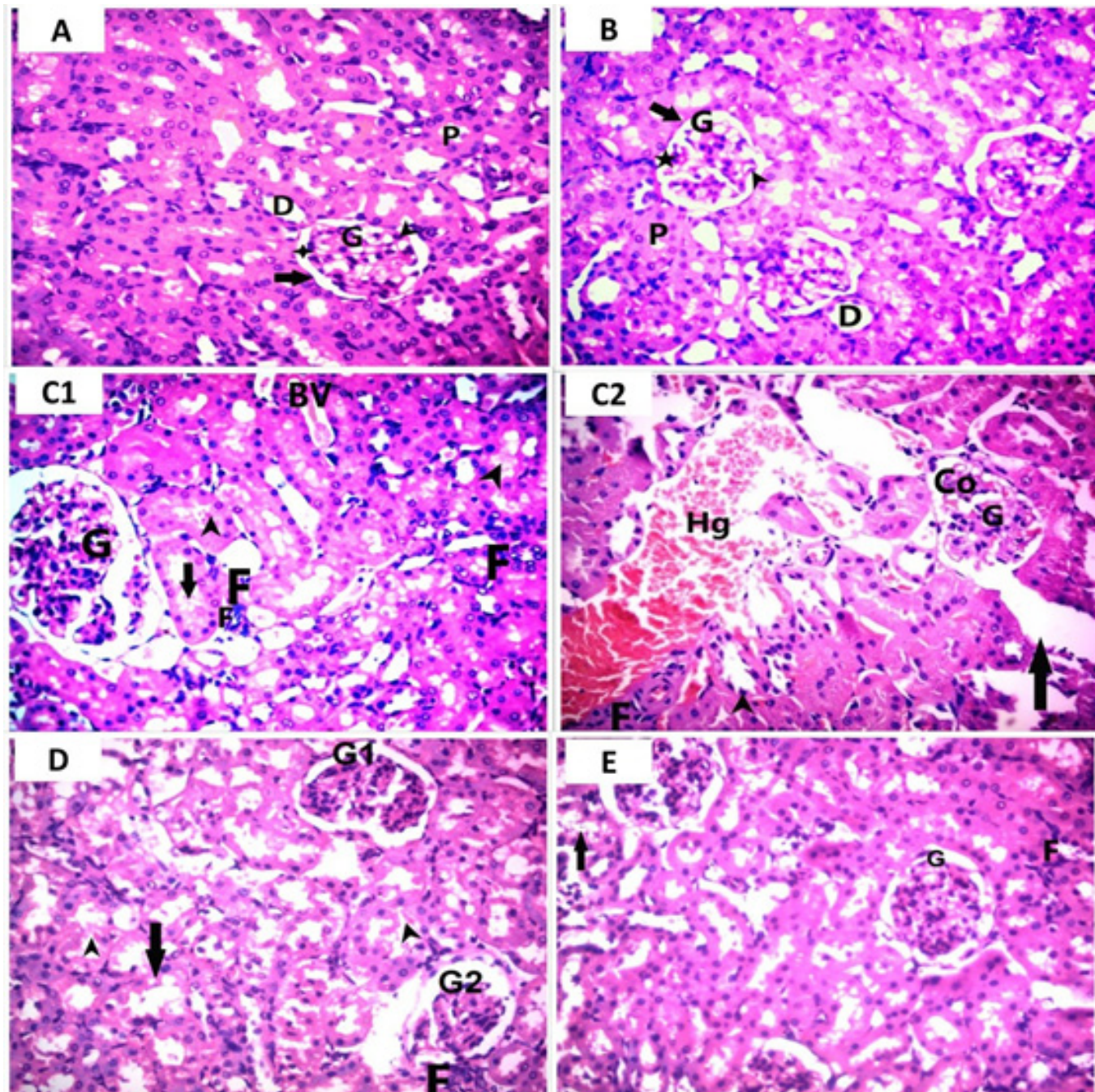


Fig. 1: A photomicrograph of H & E stained sections of rat renal cortex of different groups (A-E):

(A & B): control & dates treated groups (group I & group II) showing glomeruli (G) of normal structure surrounded by a capsule composed of parietal layer lined by simple squamous epithelium (arrow) and visceral layer lined by podocytes (arrow head) with distinct capsular space (star) in between. Proximal convoluted tubules (P) with narrow lumen are lined by pyramidal cells and distal convoluted tubules (D) with wide lumen are lined by simple cubical cells.

(C1 & C2): Aflatoxin treated subgroup (subgroup IIIa). (C1): showing apparently enlarged glomerulus (G) with segmentation of its tufts and apparently increased capsular space. Disorganized distal convoluted tubules (arrow) are noticed. Some tubules show tubular necrosis with intratubular epithelial debris (arrow head). Congested blood vessel (BV) is seen. Cellular infiltration (F) in the interstitium are also seen. (C2): showing degenerated glomerulus (G) with intraglomerular congestion (Co), massive loss of renal tubules (arrow) and other tubules with pyknotic nuclei (arrow head). Cellular infiltration (F) and massive interstitial hemorrhage (Hg) are also seen.

(D): recovery subgroup (subgroup IIIb) showing one glomerulus mildly degenerated (G1), another degenerated glomerulus with partial damaged renal capsule (G2). Disorganization of renal tubules (arrow) show vacuolations and are lined by darkly stained nuclei. Some tubules show tubular necrosis with intratubular epithelial debris (arrow head) and cellular infiltration (F) beside the glomerulus are seen.

(E): Aflatoxin and dates treated group (group IV) showing mildly degenerated glomerulus (G) and mild disorganization of renal tubules (arrow). Mild cellular infiltration (F) is found in the interstitium. (H&E x 400).

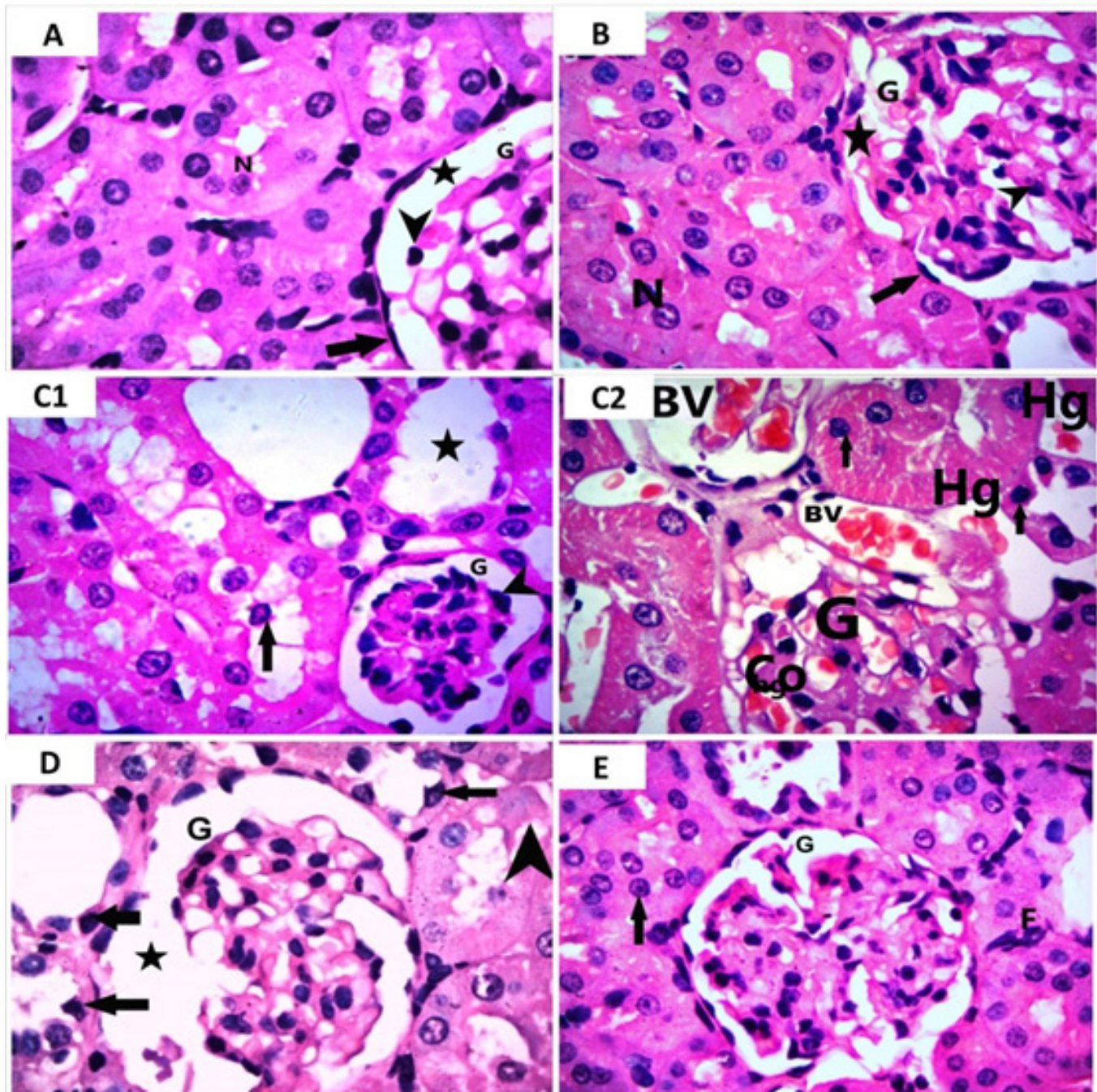


Fig. 2: A photomicrograph of H & E stained sections of rat renal cortex of different groups (A-E):
(A & B): control & dates treated groups (group I & group II) showing a glomerulus (G) of normal structure surrounded by capsule has parietal layer lined by simple squamous epithelium (arrow) and visceral layer lined by podocytes (arrow head) with distinct capsular space (star). Proximal convoluted tubules with narrow lumen lined by pyramidal cells with vesicular nuclei (N) are seen.
(C1 & C2): Aflatoxin treated subgroup (subgroup IIIa). (C1): showing degenerated glomerulus (G) with darkly stained nuclei of podocytes (arrow head). Disorganization of renal tubule with some cells showing darkly stained pyknotic nuclei invade the lumen of the tubule (arrow). Cytoplasm of these tubules are vacuolated. Other dilated tubule (star) with irregular epithelial lining with pyknotic nuclei are seen. (C2): showing glomerulus (G) with dilated capillaries and intraglomerular congestion (Co). Degenerated renal tubules are lined by cells with small pyknotic nuclei (arrows). Interstitial hemorrhage (Hg) & congested blood vessel (BV) are also seen.
(D): recovery subgroup (subgroup IIIb) showing degenerated glomerulus (G) with apparently increased capsular space (star). Disorganization of renal tubules lined by cells with darkly stained nuclei (arrows) and partially loss of epithelial lining in another tubule (arrow head) are seen.
(E): Aflatoxin and dates treated group (group IV) showing mildly degenerated glomerulus (G) and renal tubules which are lined by cells with vesicular nuclei (arrow). Mild cellular infiltrations (F) in the interstitium are seen. (Hx.&E x 1000).

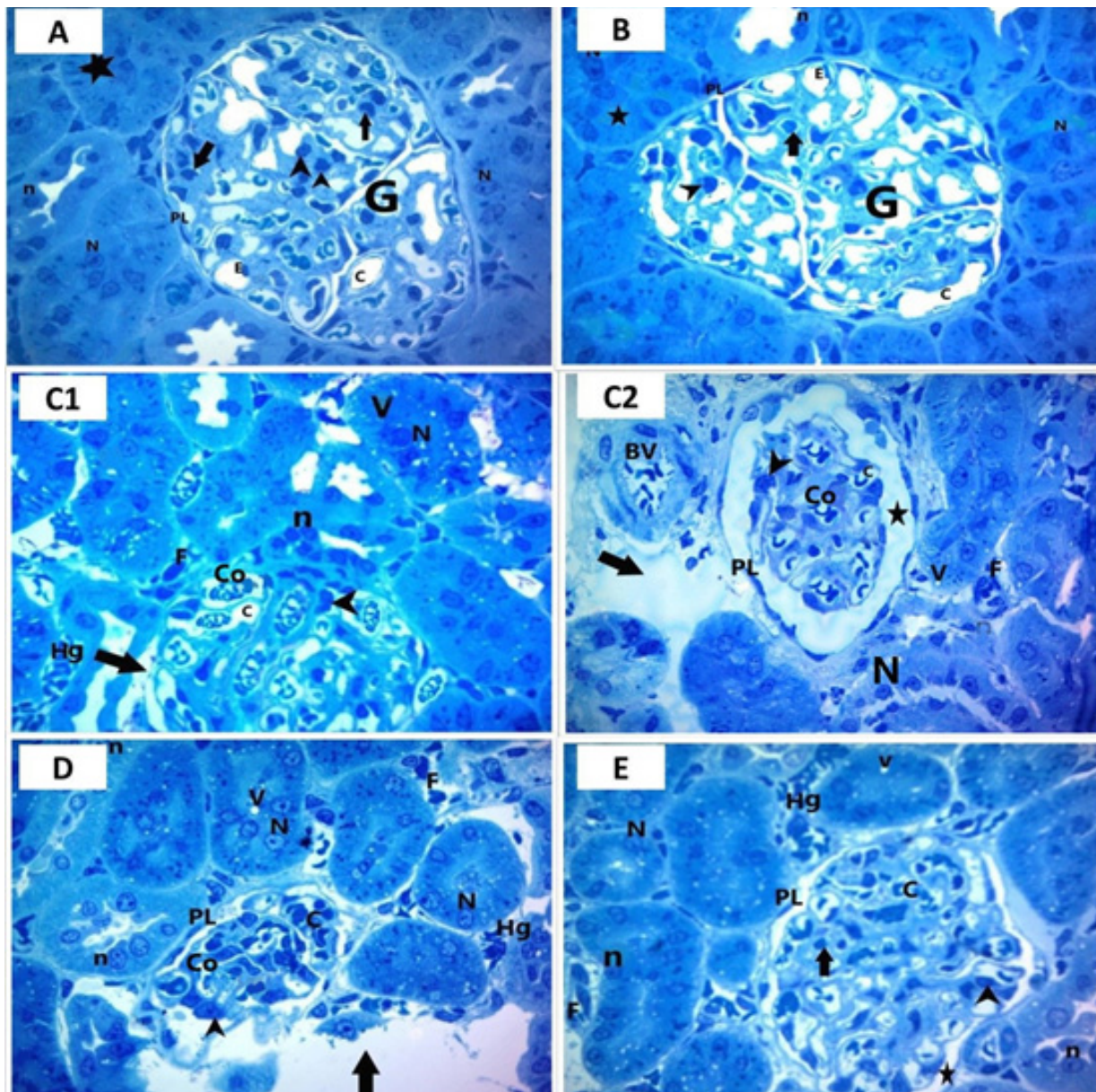


Fig. 3: A photomicrograph of toluidine blue stained sections of rat renal cortex of different groups (A-E):
 (A & B): control & dates treated groups (group I & group II) showing glomerulus (G) with capillaries (C) lined by endothelial cells (E), the spaces between the capillaries contain mesangial cells (arrow), the glomerulus is surrounded by parietal layer (PL) lined by flattened cells and visceral layer lined by podocytes (arrow head). The proximal tubules are lined by pyramidal cells with vesicular nuclei (N) and show basal striations (star). The distal tubules are lined by cubical cells with vesicular nuclei (n). There is minimal interstitial space in between the tubules.
 (C1 & C2): Aflatoxin treated subgroup (subgroup IIIa). (C1): showing glomerulus with dilated capillaries (C) showing congestion (Co), disorganized renal capsule (arrow) lined by parietal layer with loss of the flattened cells and visceral layer with apparently enlarged podocytes (arrow head). The proximal tubules are lined by pyramidal cells with darkly stained nuclei (N) and distal tubules lined by cubical cells with darkly stained nuclei (n). The cells of tubules show cytoplasmic vacuoles (V). Wide interstitial space in between the tubules shows hemorrhage (Hg) and cellular infiltration (F). (C2): showing glomerulus with capillaries (C) showing congestion (Co), the capsule is lined by parietal layer (PL) with flattened nuclei and visceral layer with apparently enlarged podocytes (arrow head). Dilated capsular space (star) is seen. The cells of tubules are lined by darkly stained nuclei (N) and show vacuolations (V). Wide interstitial space (arrow) between the tubules is seen. Cellular infiltration (F) and congested blood vessel (BV) are seen.
 (D): recovery subgroup (subgroup IIIb) showing glomerulus with capillaries (C) showing congestion (Co), with partially damaged renal corpuscle lined by parietal layer with flattened nuclei (PL) and visceral layer with apparently enlarged podocytes (arrow head). The proximal tubules lined by pyramidal cells with vesicular nuclei (N) and distal tubules lined by cubical cells with vesicular nuclei (n). The cells of tubules show cytoplasmic vacuoles (V). Wide interstitial space in between the tubules shows cellular infiltration (F) and hemorrhage (Hg). Loss of renal tissue (arrow) is observed.
 (E): Aflatoxin and dates treated group (group IV) showing glomerulus with capillaries (C) with less congestion, the glomerulus is surrounded by parietal layer with flattened nuclei (PL) and visceral layer with podocytes (arrow head) with minimal capsular space (star) in between. The proximal tubules lined by cells with vesicular nuclei (N) and distal tubules lined by cells with vesicular nuclei (n). The cells of tubules show cytoplasmic vacuoles (V). Wide interstitial space in between the tubules shows mild cellular infiltration (F) and hemorrhage (Hg) (Toluidine blue x 1000).

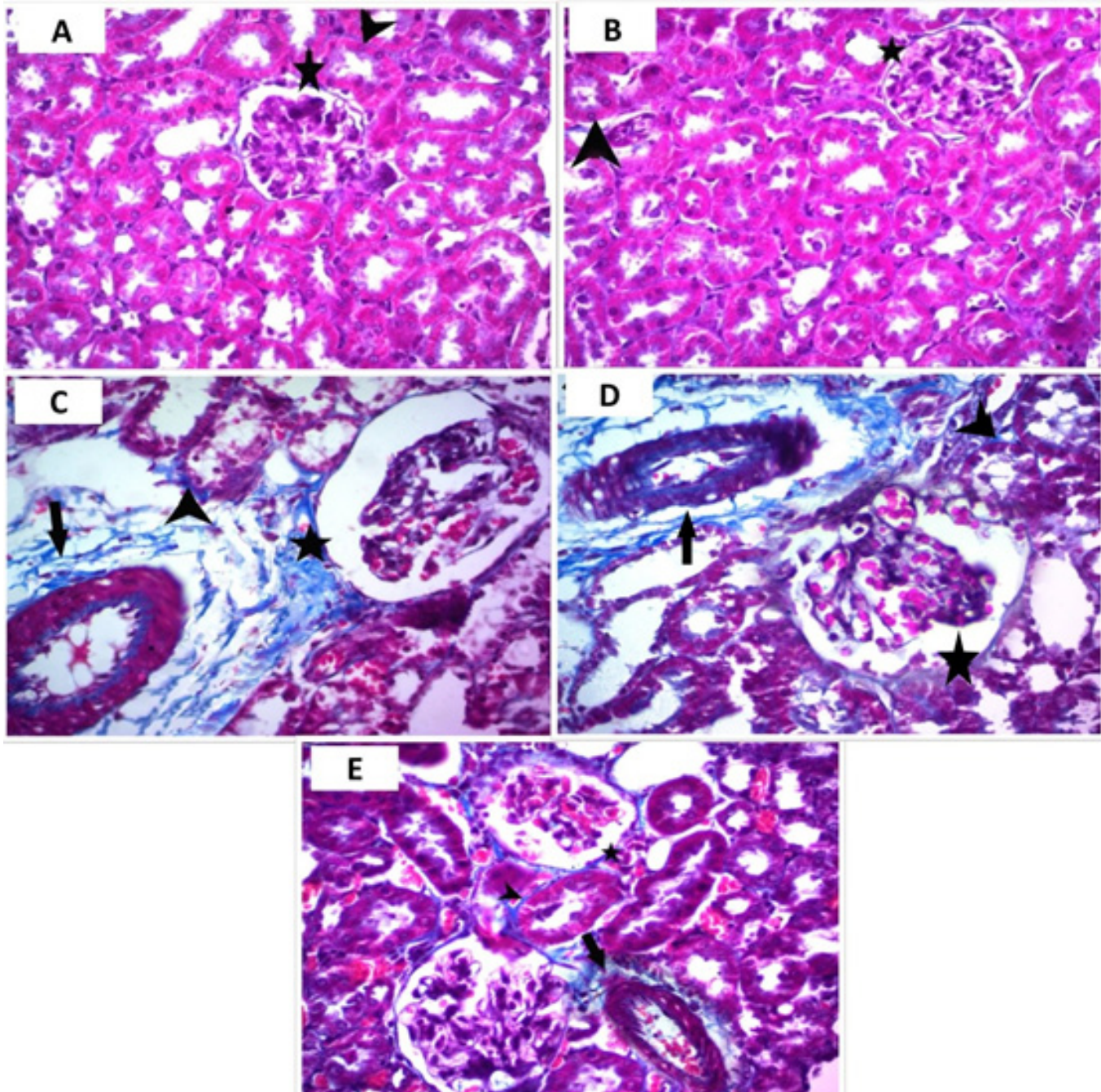


Fig. 4: A photomicrograph of Mallory Trichrome stained sections of rat renal cortex of different groups (A-E):

(A & B): control & dates treated groups (group I & group II) showing minimal amount of collagenous fibers around Bowman's capsule (star) and renal tubules (arrow head).

(C): Aflatoxin treated subgroup (subgroup IIIa) showing massive amount of collagenous fibers around Bowman's capsule (star), basement membrane of renal tubules (arrow head) and around dilated congested blood vessel (arrow).

(D): recovery subgroup (subgroup IIIb) showing moderate amount of collagenous fibers around Bowman's capsule (star), basement membrane of renal tubules (arrow head) and around dilated congested blood vessel (arrow).

(E): Aflatoxin and dates treated group (group IV) showing mild amount of collagenous fibers around Bowman's capsule (star), basement membrane of renal tubules (arrow head) and around congested blood vessel (arrow). (M.T X 400).

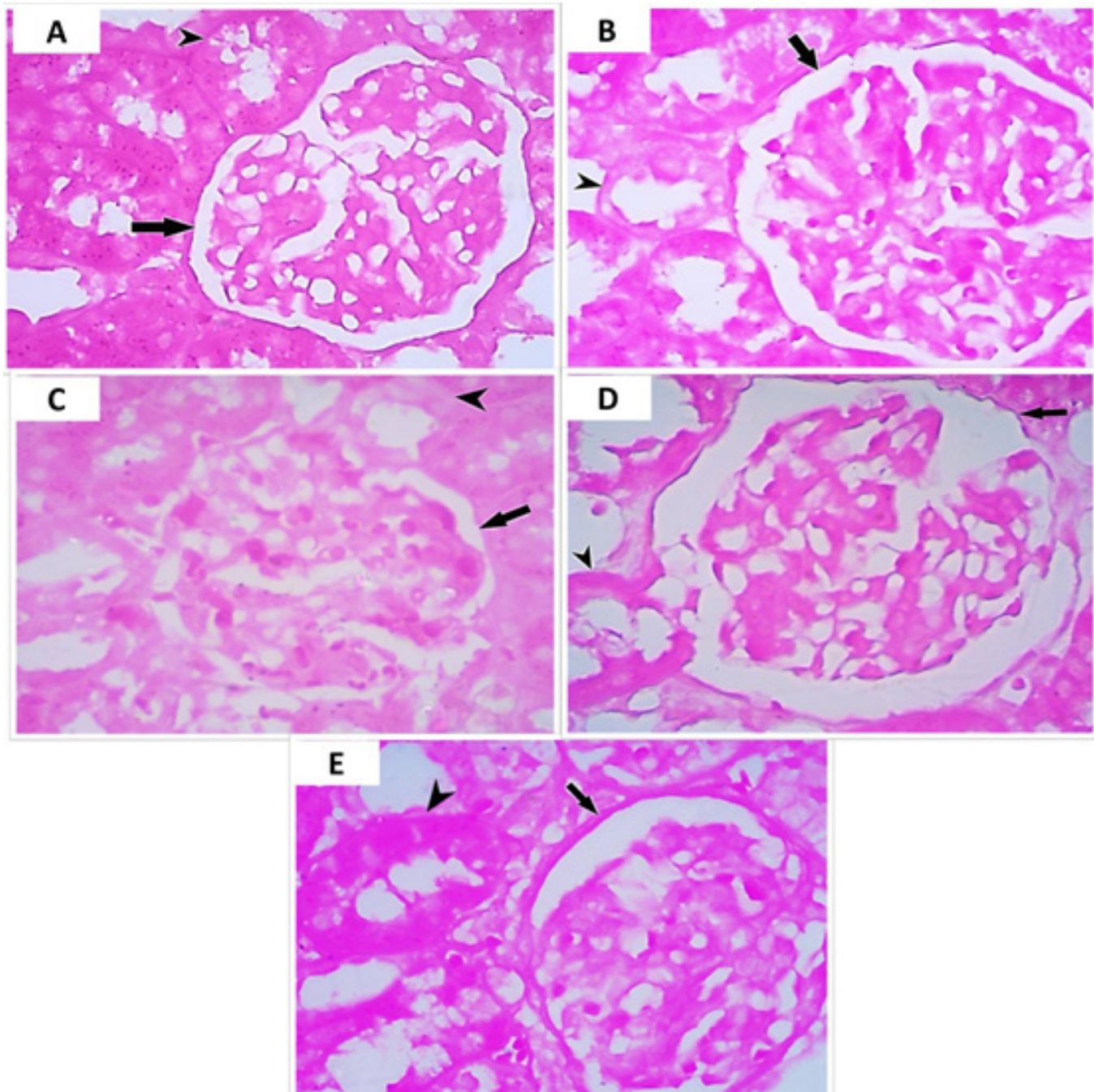


Fig. 5: A photomicrograph of PAS stained sections of rat renal cortex of different groups (A-E):
(A & B): control & dates treated groups (group I & group II) showing intense PAS reaction in both Bowman's capsule (arrow) and basement membrane of renal tubules (arrow head).
(C): Aflatoxin treated subgroup (subgroup IIIa) showing weak PAS reaction in both Bowman's capsule (arrow) and basement membrane of renal tubules (arrow head).
(D): recovery subgroup (subgroup IIIb) showing mild PAS reaction in both Bowman's capsule (arrow) and basement membrane of renal tubules (arrow head).
(E): Aflatoxin and dates treated rat (group IV) showing moderate PAS reaction in both Bowman's capsule (arrow) and basement membrane of renal tubules (arrow head).
(PAS X 1000).

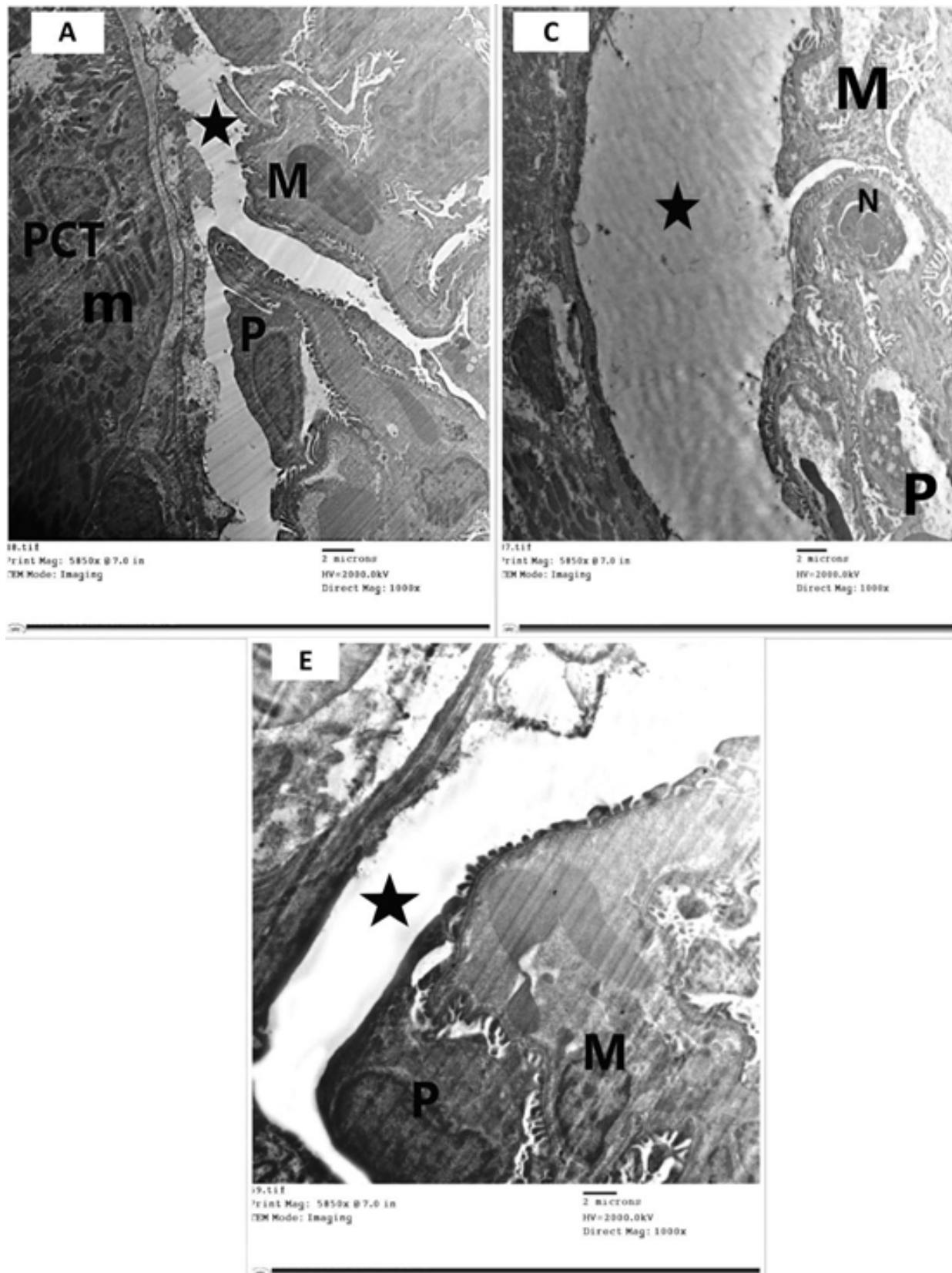


Fig. 6: An electron micrograph of rat renal cortex of some groups (A-C-E) showing capsular space of:
(A): control group (group I) showing distinct capsular space (star), podocyte (P) with euchromatic nucleus, mesangial cell (M) with euchromatic nucleus. Proximal convoluted tubule (PCT) shows cells with euchromatic nucleus and many elongated basal mitochondria (m).
(C): Aflatoxin treated subgroup (subgroup IIIa) showing dilated capsular space (star). Neutrophil cell (N) with darkly stained nuclei. Irregular shaped mesangial cell (M) and cytoplasmic vacuolations of podocyte (P) are seen.
(E): Aflatoxin and dates treated group (group IV) showing apparently less capsular space (star) than the Aflatoxin treated group. Apparently normal mesangial cell (M) with euchromatic nucleus and slightly large podocyte (P) are seen. (TEM X 1000).

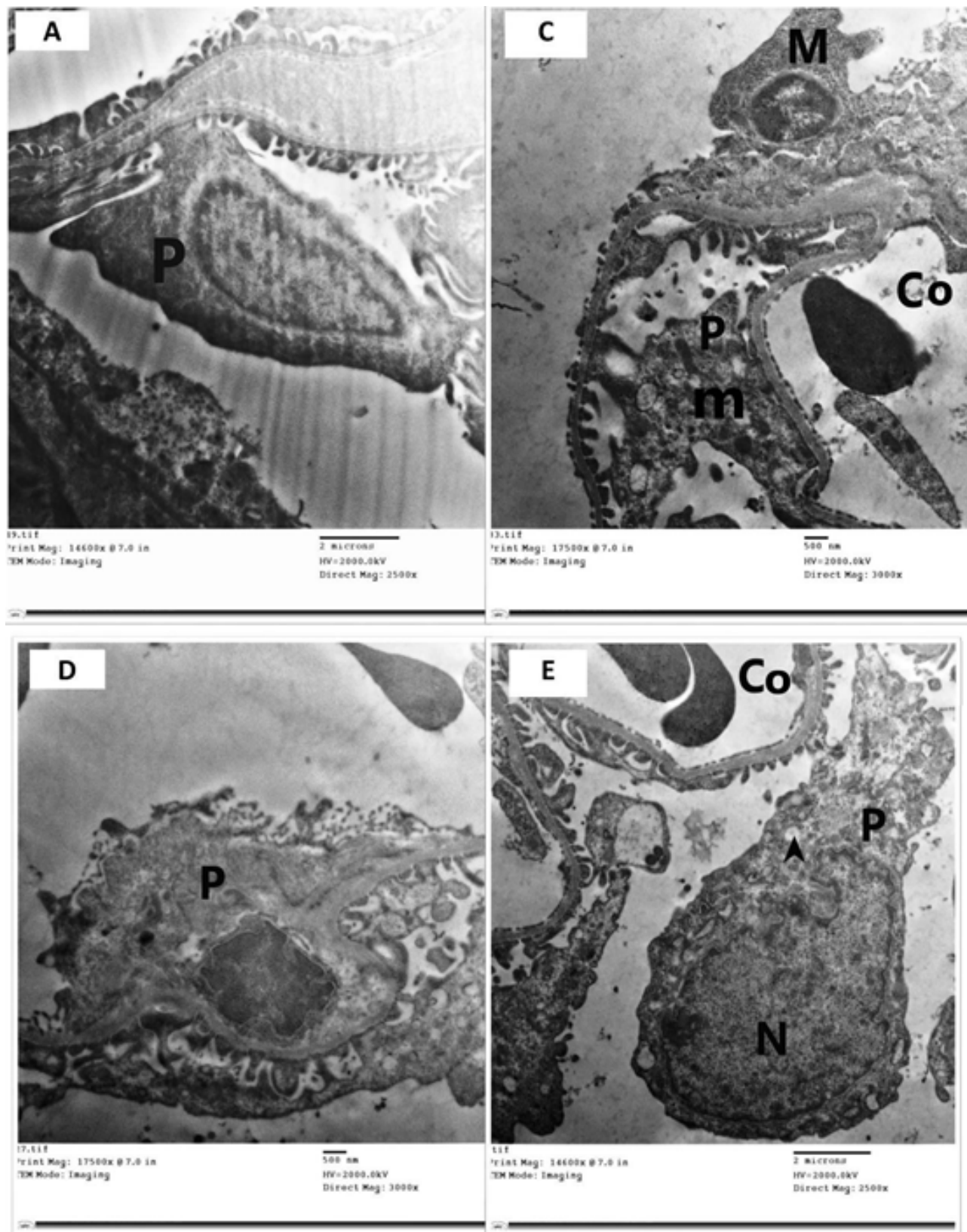


Fig. 7: An electron micrograph of rat renal cortex of some groups (A-C-D-E) showing:
 (A): control group (group I) with normal shaped podocyte (P) having euchromatic nucleus. (TEM X 2500).
 (C): Aflatoxin treated subgroup (subgroup IIIa) with irregular shaped podocyte (P) having loss of its nucleus, degenerated mitochondria (m) and rarified cytoplasm. Irregular shaped mesangial cell (M) with shrunken pyknotic nucleus is seen. Intraglomerular congestion (Co) is observed. (TEM X 3000).
 (D): recovery subgroup (subgroup IIIb) with irregular shaped podocyte (P) having darkly stained nucleus. (TEM X 3000).
 (E): Aflatoxin and dates treated group (group IV) apparently enlarged podocyte (P) having large irregular shaped nucleus (N) and vacuolated cytoplasm (arrow head). Intraglomerular congestion is seen (Co). (TEM X 2500).

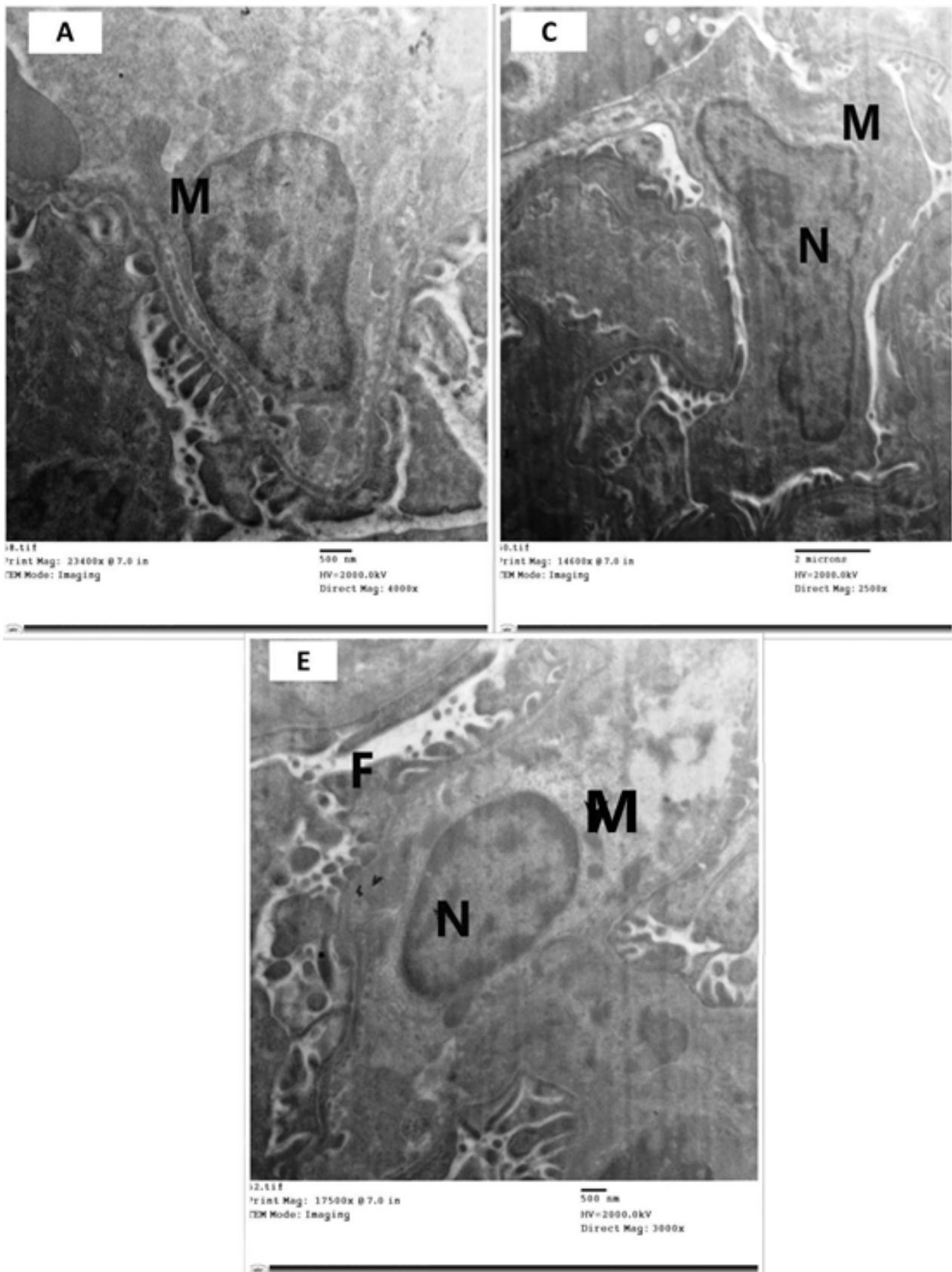


Fig. 8: An electron micrograph of rat renal cortex of some groups (A-C-E) showing:
(A): control group (group I) with normal shaped cell mesangial cell (M) having euchromatic nucleus. (TEM X 4000).
(C): Aflatoxin treated subgroup (subgroup IIIa) showing irregular shaped mesangial cell (M) with irregular shaped nucleus (N). (TEM X 2500).
(E): Aflatoxin and dates treated group (group IV) showing slightly normal shaped mesangial cell (M) with euchromatic nucleus (N). Large fused podocyte foot processes (F) are seen. (TEM X 3000).

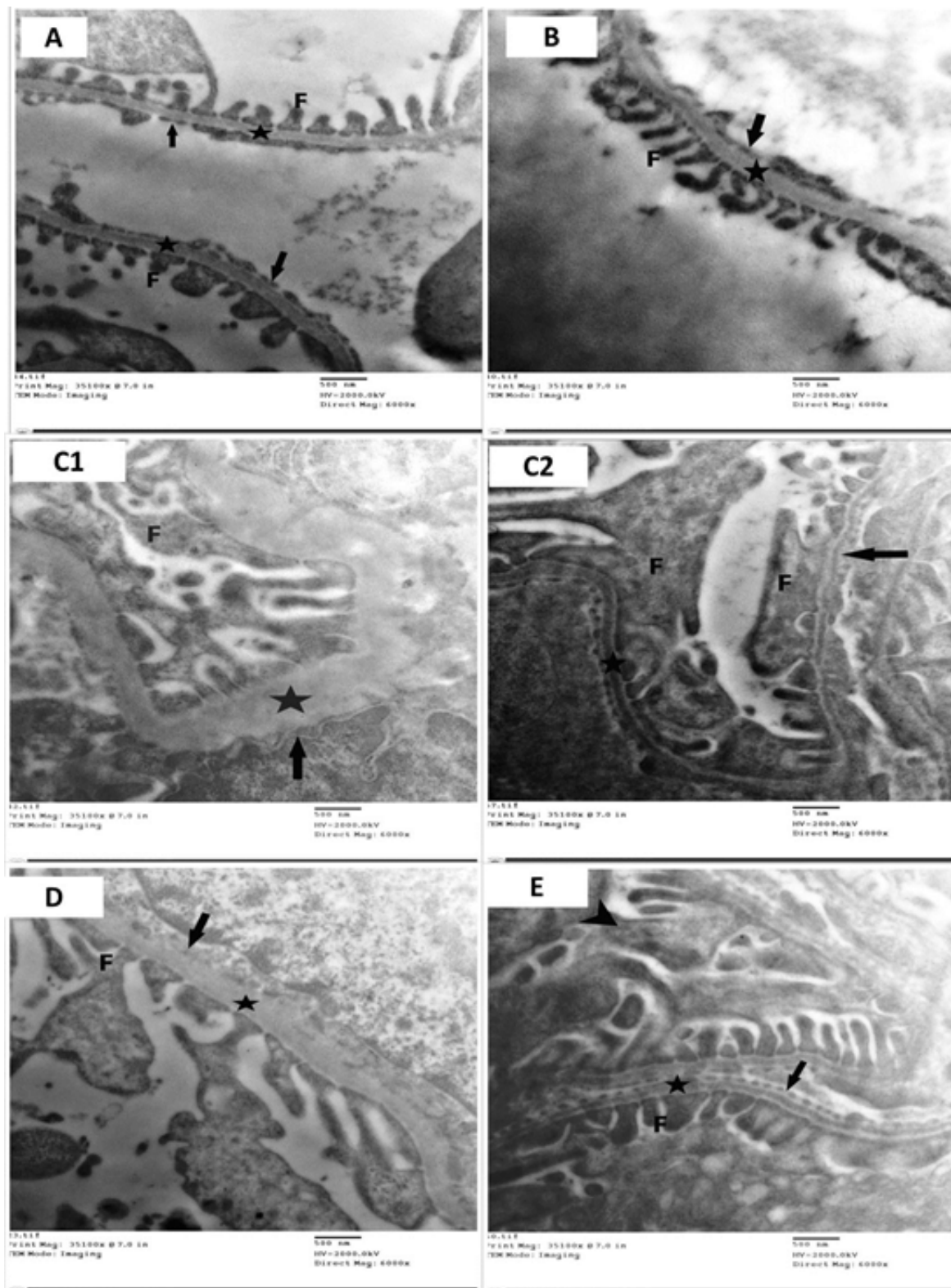


Fig. 9: An electron micrograph of rat renal cortex of different groups (A-E) showing the blood renal barrier of :
 (A & B): control & dates treated groups (group I & group II) with distinct glomerular basement membrane (star), non-fused podocyte foot processes (F) and fenestrated endothelial cells (arrow) on the other side.
 (C1 & C2): Aflatoxin treated subgroup (subgroup IIIa). (C1): with apparently thickened glomerular basement membrane (star), distortion of the podocyte foot processes (F) and fused endothelial cells (arrow) on the other side. (C2): with loss of the typical trilaminar appearance of glomerular basement membrane (star), large fused podocyte foot processes (F) and fused endothelial cells (arrow) on the other side
 (D): recovery subgroup (subgroup IIIb) with apparently less thickening of the glomerular basement membrane (star) than that of the Aflatoxin group, distortion of the podocyte foot processes (F) and fused endothelial cells (arrow) on the other side.
 (E): Aflatoxin and dates treated rat (group IV) with apparently less thickening of the glomerular basement membrane (star) than the Aflatoxin group, non-fused podocyte foot processes (F) and fenestrated endothelial cells (arrow) on the other side. (TEM X 6000).

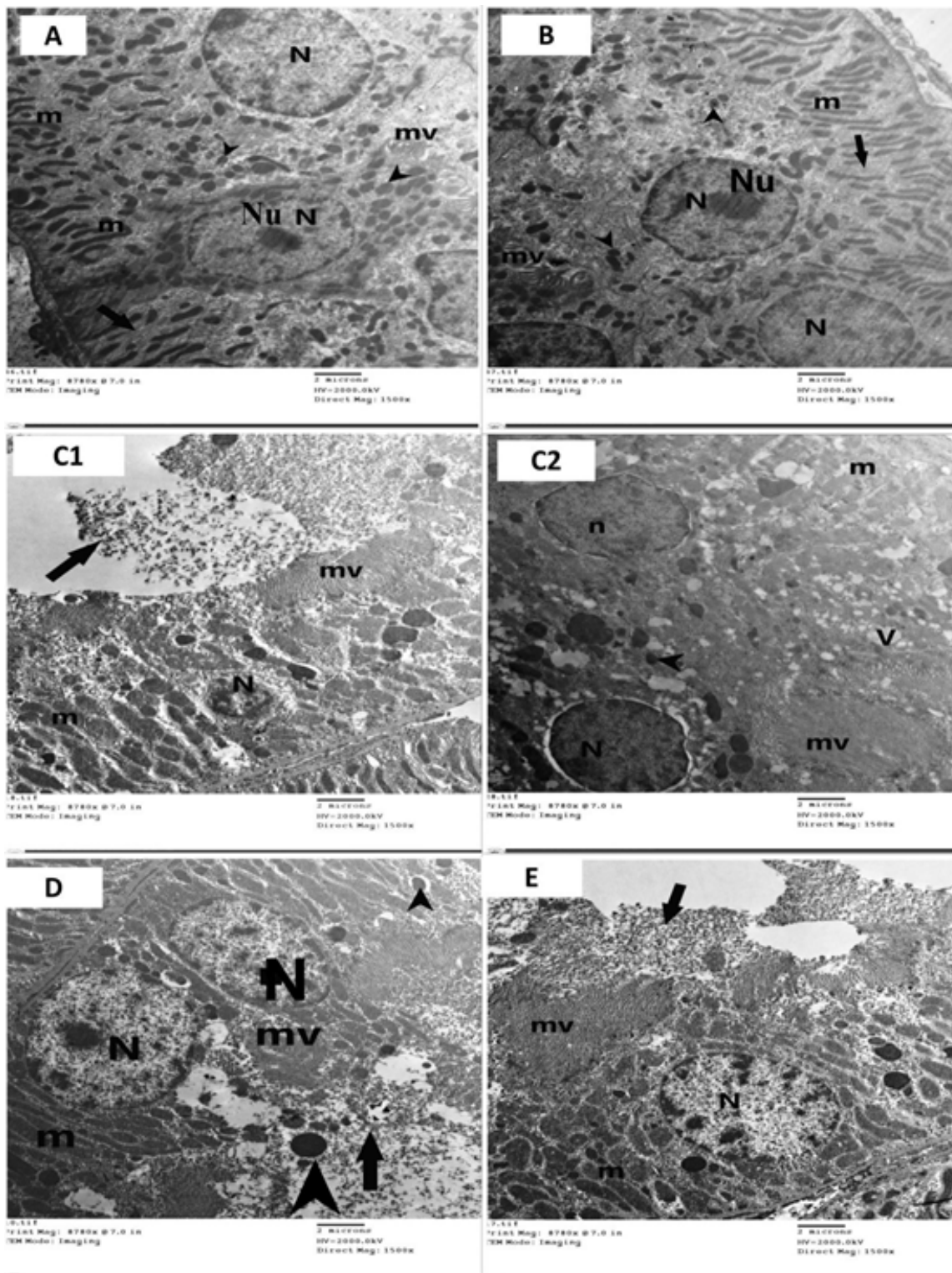


Fig. 10: An electron micrograph of rat renal cortex of different groups (A-E) showing proximal convoluted tubules (PCT) of: (A & B): control & dates treated groups (group I & group II) with cells with round euchromatic nucleus (N) with central nucleolus (Nu). Extensive basal infoldings (arrow) with many elongated basal mitochondria (m) are seen. lysosomes (arrow head) are also noticed in the cytoplasm. Long apical microvilli (mv) are seen. (C1 & C2): Aflatoxin treated subgroup (subgroup IIIa). (C1): with cells with irregular shrunken pyknotic nucleus (N), swollen mitochondria (m). Shedding cytoplasm (arrow) in the lumen and closely packed apical microvilli (mv) are noticed. (C2): with Cells with euchromatic nucleus (n) and other cells heterochromatic nucleus (N), both have dilated prenuclear space. There are swollen mitochondria (m), multiple cytoplasmic vacuoles (V) and multiple lysosomes (arrow head). Closely packed apical microvilli (mv) are also seen. (D): recovery subgroup (subgroup IIIb) with cells having euchromatic nuclei (N). Abnormal shaped mitochondria (m) are noticed. Multiple lysosomes (arrow head) are seen. There are closely packed apical microvilli (mv) and shedding cytoplasm (arrow) in the lumen. (E): Aflatoxin & dates treated group (group IV) with cells having euchromatic nucleus (N). There are swollen mitochondria (m). Long apical microvilli (mv) and shedding cytoplasm (arrow) in the lumen are seen. (TEM X 1500).

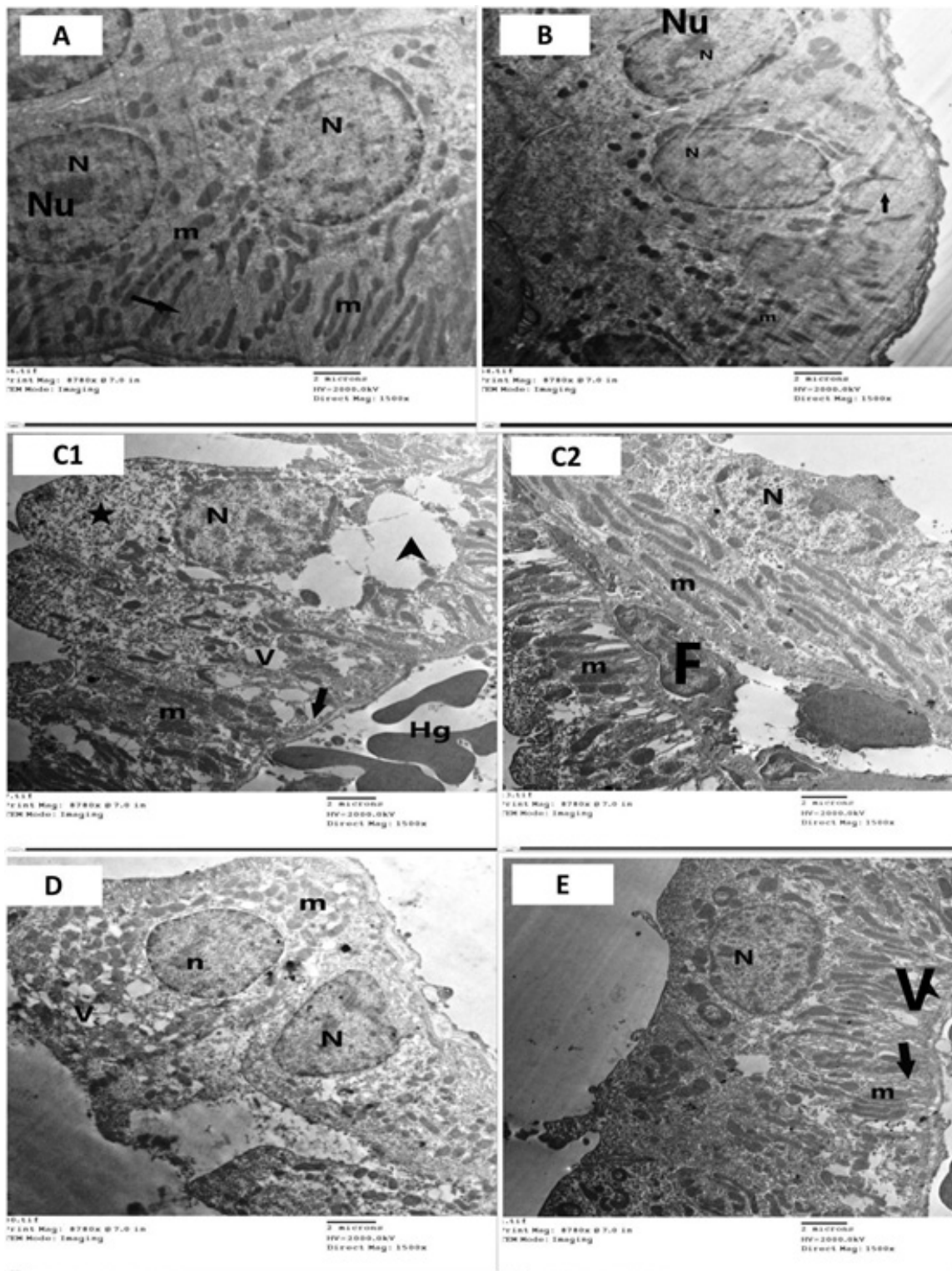


Fig. 11: An electron micrograph of rat renal cortex of different groups (A-E) showing distal convoluted tubules (DCT) of: (A & B): control & dates treated groups (group I & group II) with cells with apical round euchromatic nucleus (N) with central nucleolus (Nu). Many basal infoldings (arrow) are noticed with numerous elongated mitochondria (m) in between. No apical microvilli are seen. (C1 & C2): Aflatoxin treated subgroup (subgroup IIIa). (C1): with cells with euchromatic nucleus (N) displaced more apically and loss of basal infoldings (arrow) with abnormal distributed mitochondria (m). Fused cytoplasmic vacuoles (arrow head) and other multiple small cytoplasmic vacuoles (V) are seen. Rarefaction of the cytoplasm (star) and interstitial hemorrhage (Hg) are noticed. (C2): with the cells having abnormal shaped nucleus (N) with multiple peripheral patches of heterochromatin. There are irregular distributed multiple mitochondria (m). cellular infiltration is seen in the interstitium (F). (D): recovery subgroup (subgroup IIIb) with cells with irregular euchromatic indented nucleus (N) and another nucleus (n) with pre-nuclear space. Basally located swollen mitochondria (m) and multiple cytoplasmic vacuoles (V) are seen. (E): Aflatoxin & dates treated group (group IV) with cells with an apical euchromatic nucleus (N). Basal infoldings (arrow) with apparently normal shaped regularly distributed mitochondria (m) in between. Vacuolations (V) of the cytoplasm are seen. (TEM X 1500).

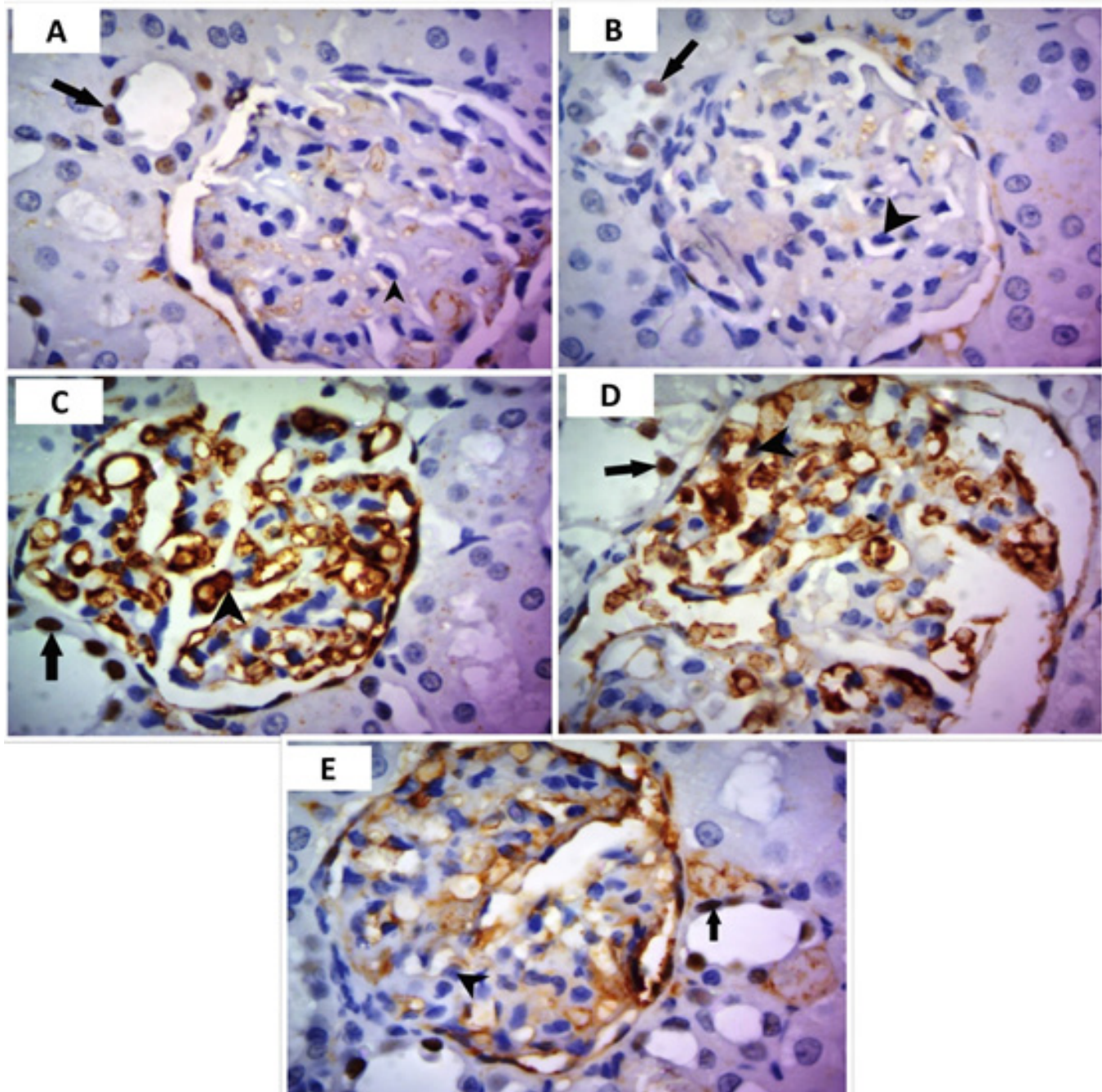


Fig. 12: A photomicrograph of immune stained (PAX 2) sections of rat renal cortex of different groups (A-E):
(A & B): control & dates treated groups (group I & group II) showing intense expression of PAX2 in nuclei of distal tubules (arrow) but negative expression in nuclei of podocytes (arrow head).
(C): Aflatoxin treated subgroup (subgroup IIIa) showing intense expression of PAX2 in nuclei of both podocytes (arrow head) and distal tubules (arrow).
(D): recovery subgroup (subgroup IIIb) showing moderate expression of PAX2 in nuclei of both podocytes (arrow head) and distal tubules (arrow).
(E): Aflatoxin and dates treated group (group IV) showing mild expression of PAX2 in nuclei of both podocytes (arrow head) and distal tubules (arrow).
(PAX2 X 1000).

Statistical analysis

Statistical comparison of body weight, kidney weight, serum urea and creatinine levels in the different studied groups was carried out using the analysis of variance test. There was no significant change in the means of body and kidney weights of rats of all studied groups as compared to control group ($P > 0.05$). (Tables 1,2 & Histograms 1,2). There was no significant change in the means of body and kidney weights of rats of recovery subgroup as compared to protected group ($P > 0.05$). (Tables 3,4 & Histograms 3,4).

There was no significant increase in serum urea and creatinine level of dates group and protected group as compared to control group. While there was highly significant increase in serum urea and creatinine level observed in Aflatoxin B1 subgroup (subgroup IIIa) and recovery subgroup (subgroup IIIb) as compared to the control group ($p < 0.001$), there was highly significant decrease in mean of

serum urea and creatinine level observed in protected group (group IV) as compared to Aflatoxin B1 subgroup ($p < 0.001$) (Tables 5,6 & Histograms 5,6).

There was highly significant decrease in serum urea and creatinine level observed in protected group (group IV) as compared to recovery subgroup (subgroup IIIb) ($p < 0.001$) (Tables 7,8 & Histograms 7,8).

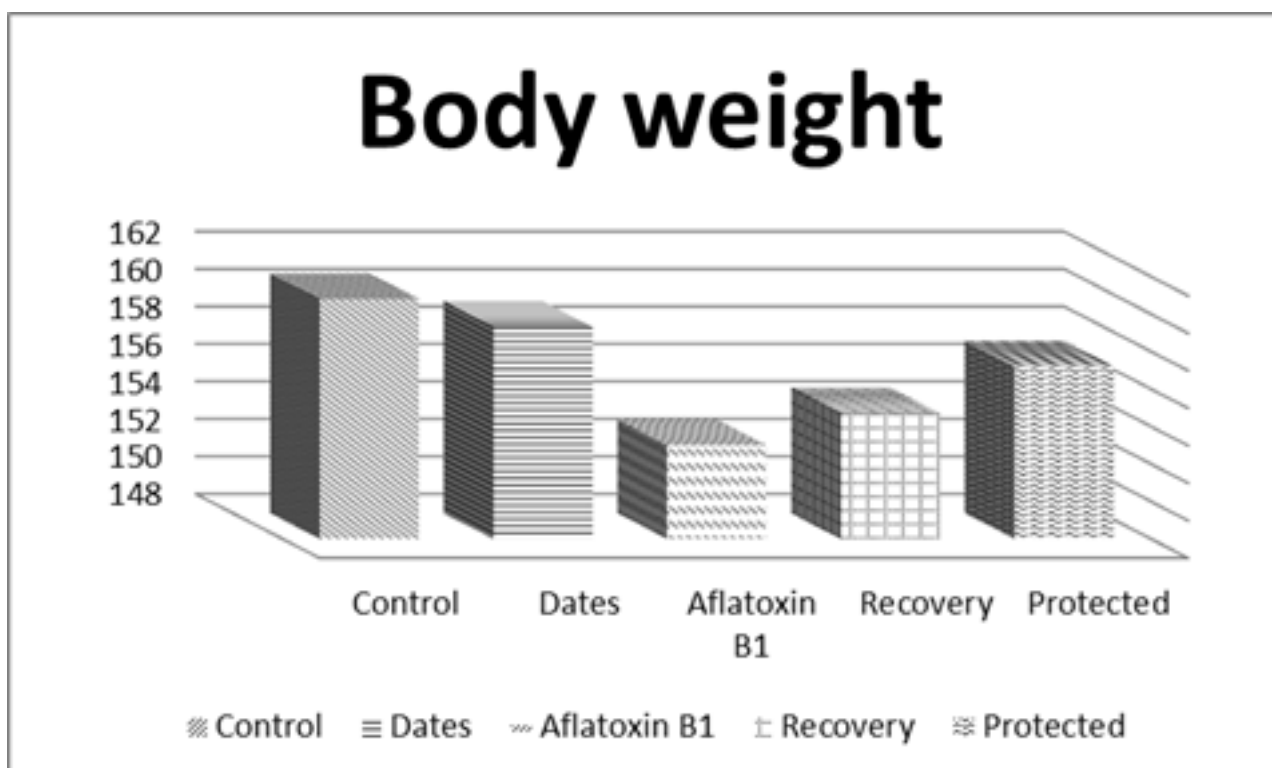
Determination of Aflatoxins concentration using HPLC-FLD

Aflatoxin B1 concentration was detected using HPLC. Diagram (1) showed the curve of the extracted Aflatoxins from the toxigenic *A. flavus* and the concentration was calculated through the comparison between the area under the curve of the standard and the sample. The concentration of AFB1 from the extracted samples was 19.8 µg/100 ml (Dig.1).

Table 1: Statistical means of body weights (gm) of various experimental groups.

Group	Mean ± SD	(Test of significance)	P- value
Group I (Control)	160.8 ± 7.9		
Group II (Dates)	159.3 ± 5.6	0.477	0.640*
Subgroup IIIa (Aflatoxin B1)	153 ± 8.5	2.083	0.055*
Subgroup IIIb (Recovery)	154.7 ± 8	1.681	0.113*
Group IV (Protected)	157.2 ± 7.3	1.030	0.319*

P value > 0.05 = Non significant.*

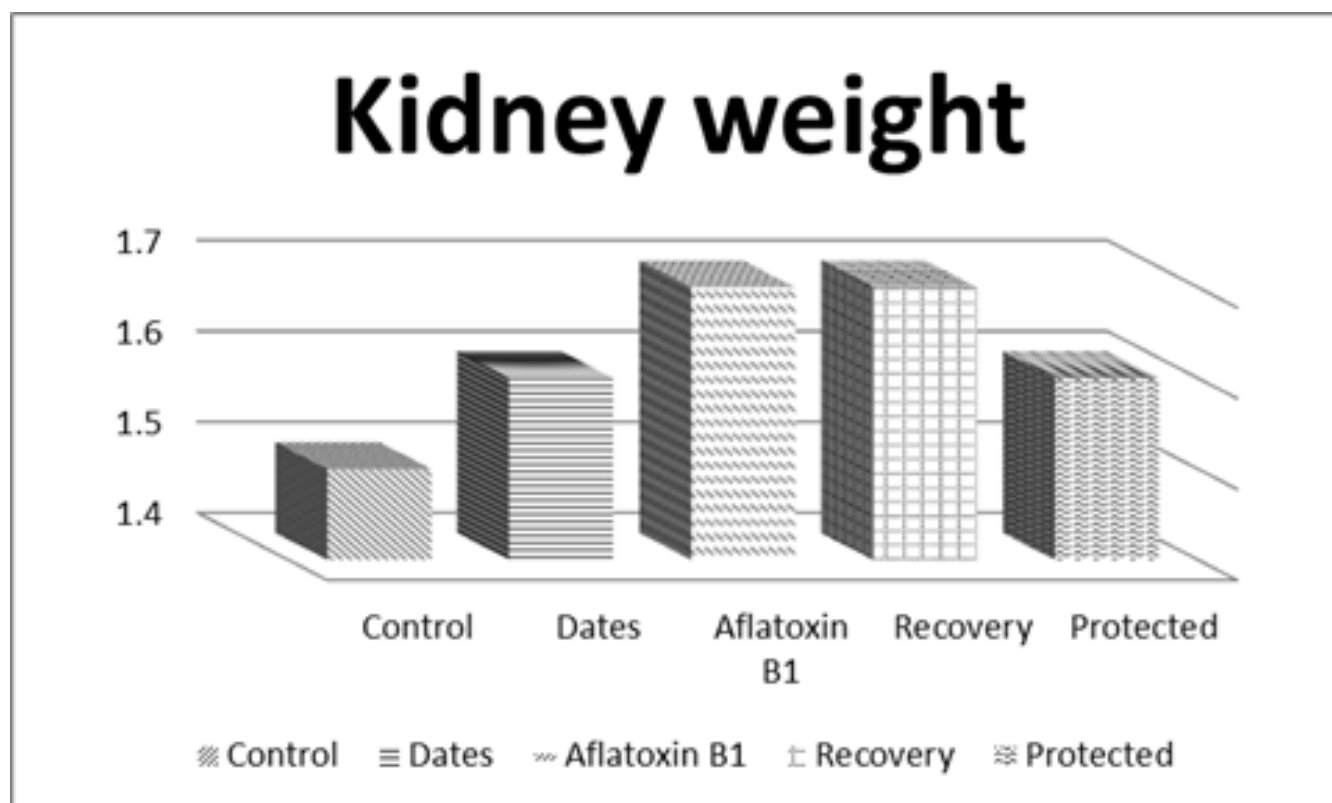


Histogram 1: Statistical means of body weights (gm) of various experimental groups.

Table 2: Statistical means of kidney weights (gm) of various experimental groups.

Group	Mean ± SD	(Test of significance)	P- value
Group I (Control)	1.5 ± 0.2		
Group II (Dates)	1.6 ± 0.2	0.781	0.447*
Subgroup IIIa (Aflatoxin B1)	1.7 ± 0.2	0.032	0.060*
Subgroup IIIb (Recovery)	1.7 ± 0.3	1.643	0.121*
Group IV (Protected)	1.6 ± 0.3	1.048	0.311*

P value > 0.05 = Non significant*.

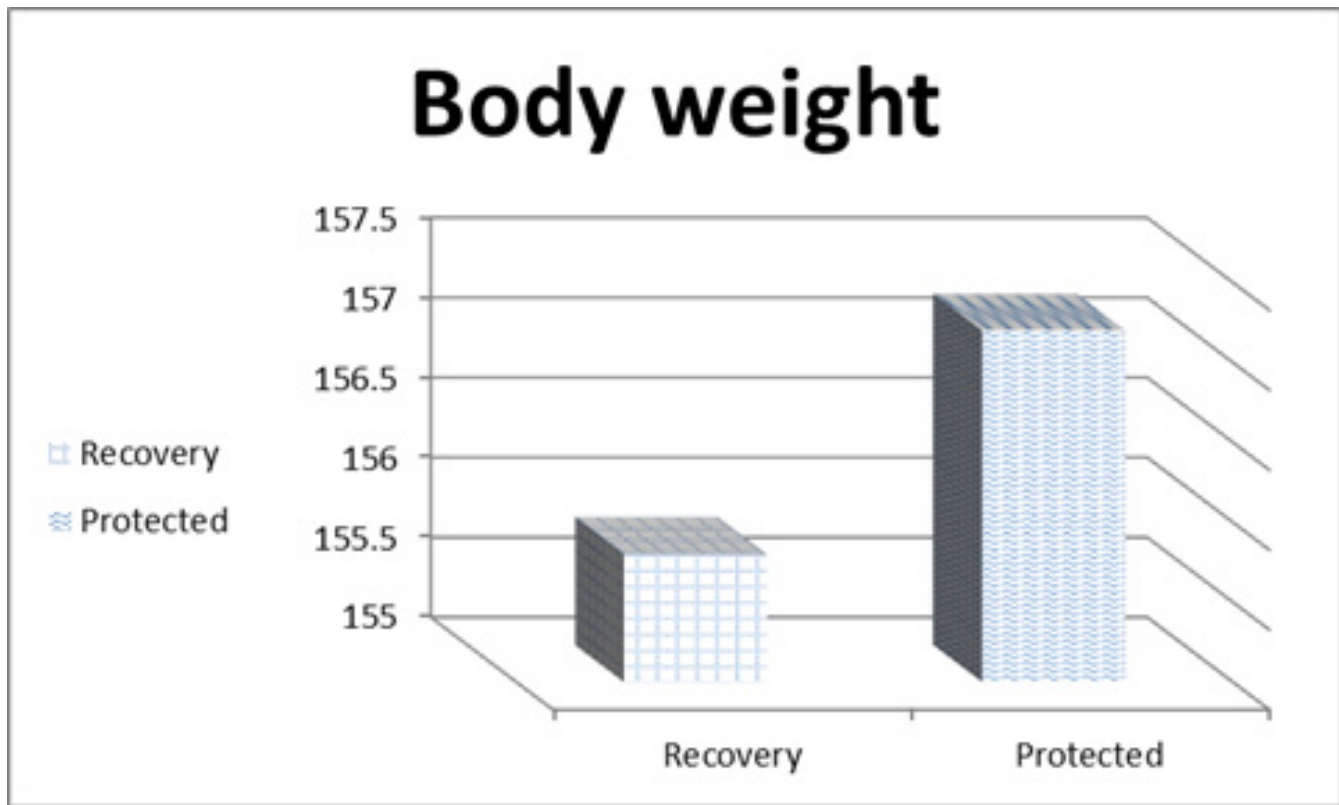


Histogram 2: Statistical means of kidney weights (gm) of various experimental groups.

Table (3): Statistical means of body weights (gm) of recovery subgroup (IIIb) versus protected group (IV).

Group	Mean ± SD	(Test of significance)	P- value
Subgroup IIIb (Recovery)	155.8 ± 7.7		
Group IV (Protected)	157.2 ± 7.3	0.414	0.685*

P value > 0.05 = Non significant*.

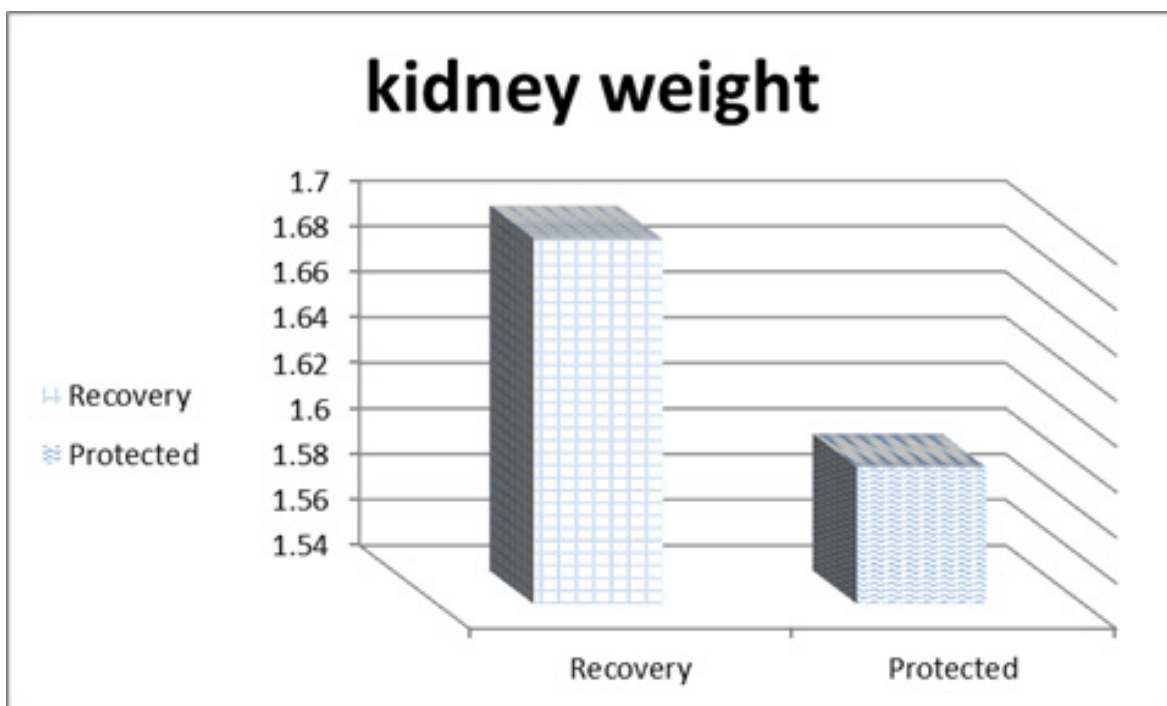


Histogram 3: Statistical means of body weights (gm) of IIIb subgroup versus IV group

Table 4: Statistical means of kidney weights (gm) of recovery subgroup (IIIb) versus protected group (IV).

Group	Mean \pm SD	(Test of significance)	<i>P</i> -value
Subgroup IIIb (Recovery)	1.7 \pm 0.3		
Group IV (Protected)	1.6 \pm 0.3	0.982	0.341*

P value > 0.05 = Non significant*.

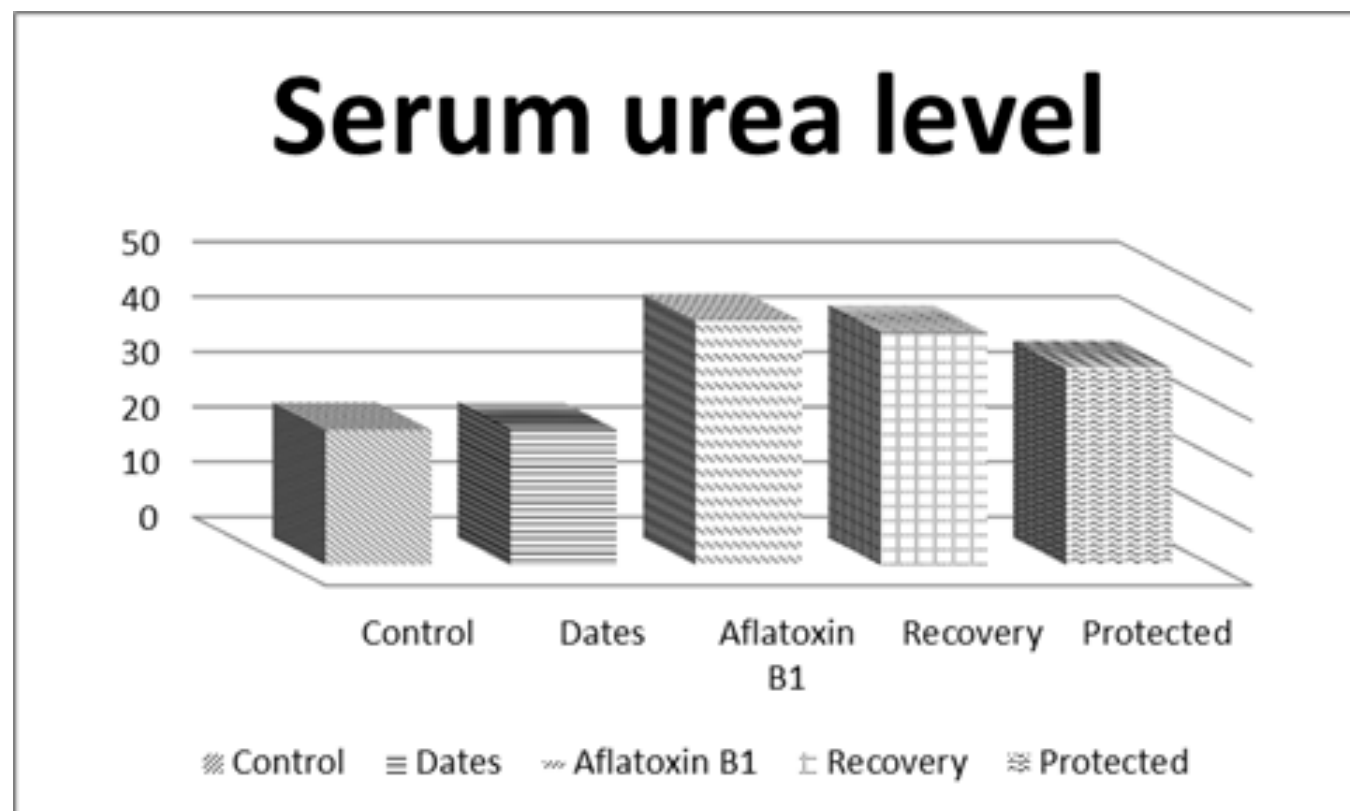


Histogram 4: Statistical means of kidney weights (gm) of IIIb subgroup versus IV group.

Table 5: Statistical means of serum urea level (mg/dl) of various experimental groups.

Group	Mean ± SD	(Test of significance)	P- value
Group I (Control)	24.5 ± 0.3		
Group II (Dates)	24.6 ± 0.3	0.043	0.966*
Subgroup IIIa (Aflatoxin B1)	44.3 ± 0.6	130.528	0.000***
Subgroup IIIb (Recovery)	42.2 ± 2.8	22.039	0.000***
Group IV (Aflatoxin & Dates)	35.8 ± 3.4	10.965	0.000***

P value > 0.05 = Non significant*.
P value < 0.001 = Highly significant***.

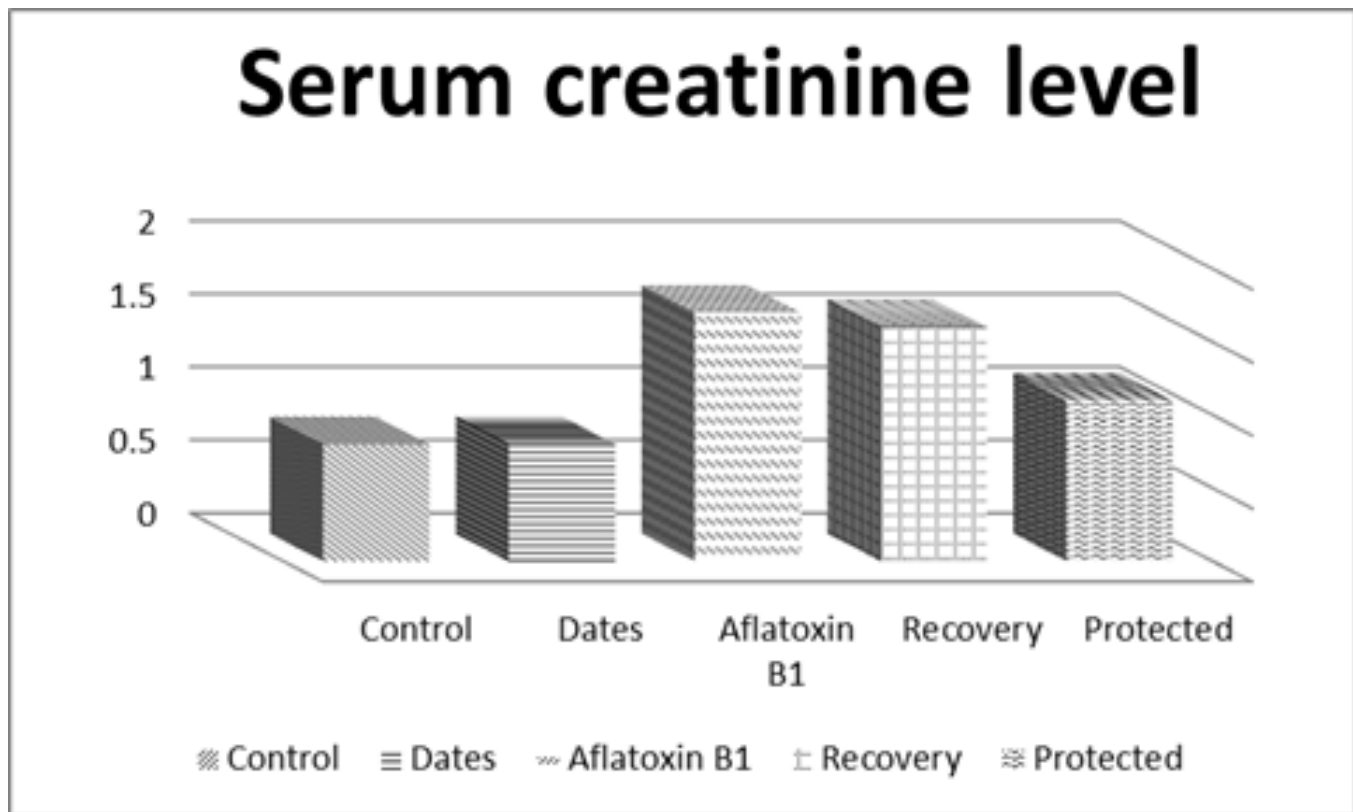


Histogram 5: Statistical means of serum urea level (mg/dl) of various experimental groups.

Table 6: Statistical means of serum creatinine level (mg/dl) of various experimental groups.

Group	Mean ± SD	(Test of significance)	P- value
Group I (Control)	0.8 ± 0.1		
Group II (Dates)	0.8 ± 0.1	0.098	0.923*
Subgroup IIIa (Aflatoxin B1)	1.7 ± 0.6	4.462	0.000***
Subgroup IIIb (Recovery)	1.6 ± 0.3	7.265	0.000***
Group IV (Aflatoxin & Dates)	1.1 ± 0.1	4.614	0.000***

P value > 0.05 = Non significant*.
P value < 0.001 = Highly significant***.

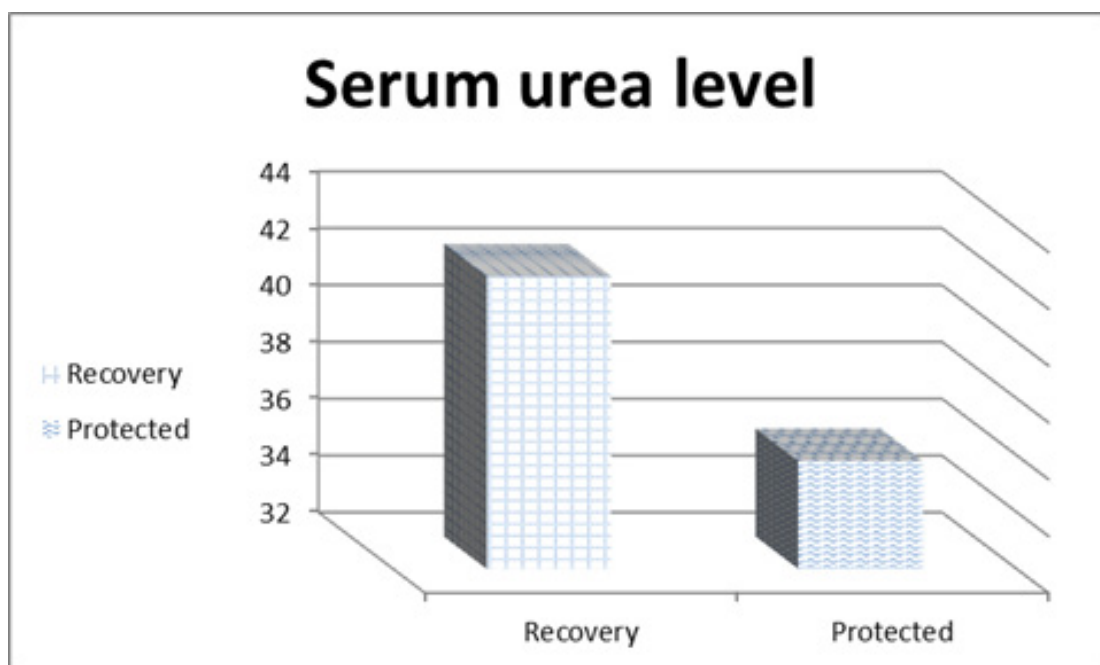


Histogram 6: Statistical means of serum creatinine level (mg/dl) of various experimental groups.

Table 7: Statistical means of serum urea level (mg/dl) of IIIb subgroup versus IV group.

Group	Mean ± SD	(Test of significance)	P- value
Subgroup IIIb (Recovery)	42.3 ± 2.9		
Group IV (Aflatoxin & Dates)	35.8 ± 3.4	4.625	0.000***

P value < 0.001 = Highly significant***.

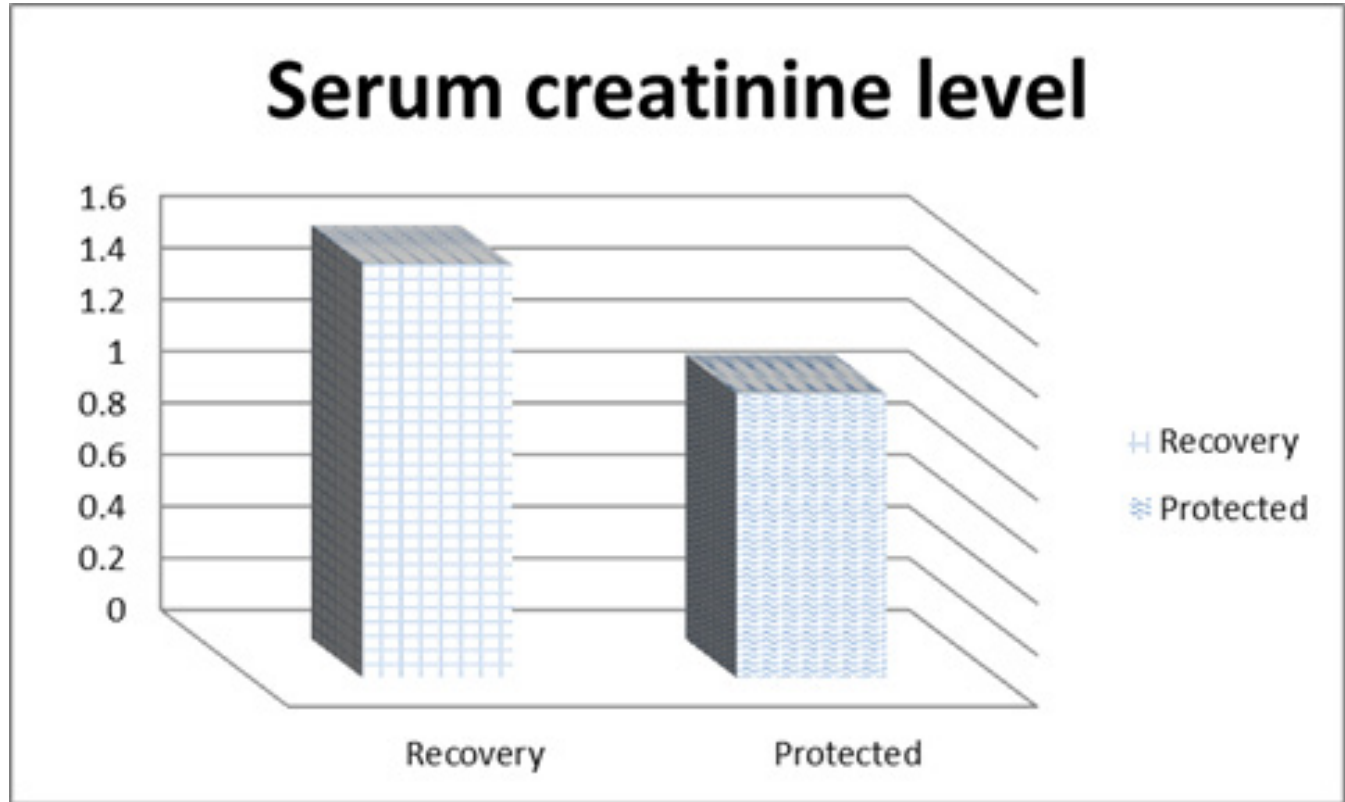


Histogram 7: Statistical means of serum urea level (mg/dl) of IIIb subgroup versus IV group.

Table 8: Statistical means of serum creatinine level (mg/dl) of IIIb subgroup versus IV group.

Group	Mean ± SD	(Test of significance)	P- value
Subgroup IIIb (Recovery)	1.6 ± 0.3		
Group IV (Aflatoxin & Dates)	1.1 ± 0.1	4.676	0.000***

P value < 0.001 = Highly significant***.



Histogram 8: Statistical means of serum creatinine level (mg/dl) of IIIb subgroup versus IV group.

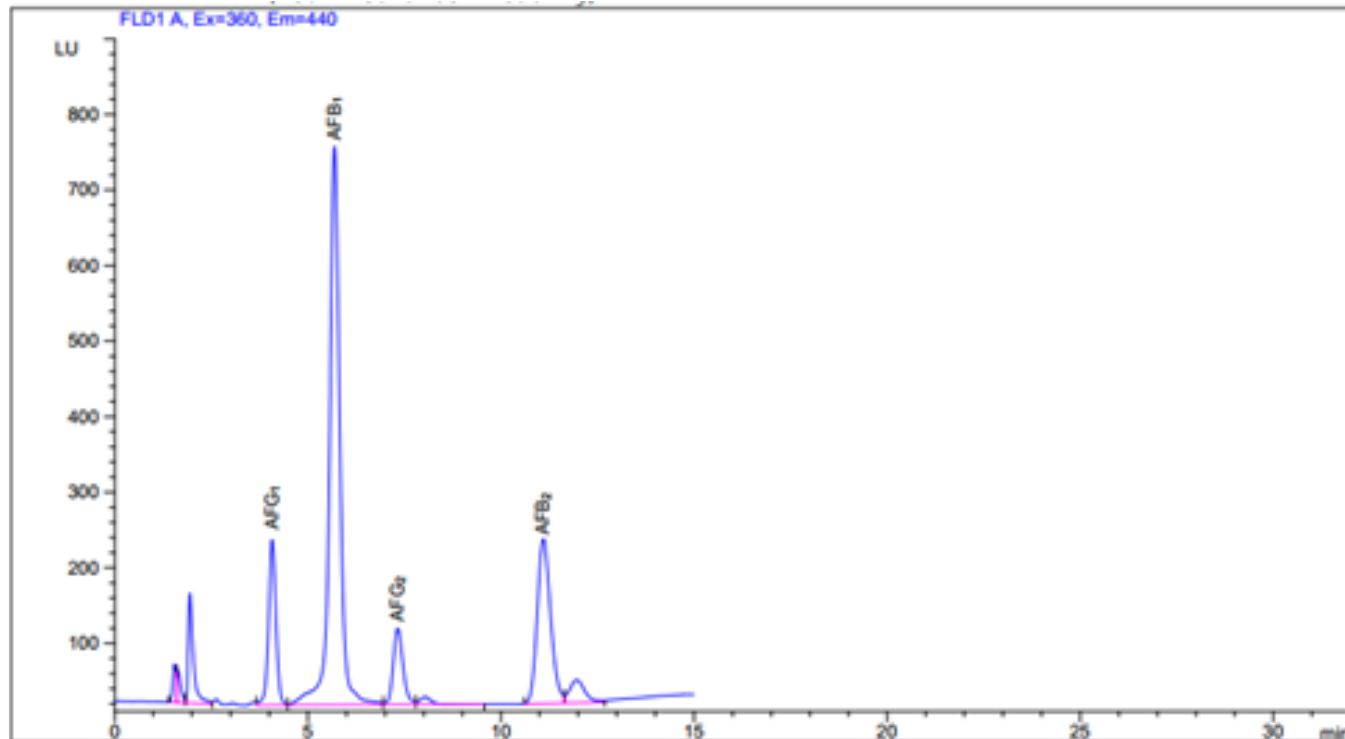


Fig. (1): Chromatogram of aflatoxins (AFG₁, AFB₁, AFG₂ and AFB₂) of the chloroform extract of toxigenic A. flavus.

DISCUSSION

In spite some previous researches proved the effective role of many food additives in relieving aflatoxicosis, few researches were done on the role of dates extract in its amelioration. We performed this study to evaluate the toxicity of Aflatoxins B1 and the possible protective role of dates^[19].

The oxidation stress was the main mechanism reported by many authors for AFB1- induced toxicity. Accordingly, antioxidants could reduce this toxicity Dates extract contains important nutrients and has antioxidant properties^[20 & 21].

The kidney was considered a potential target for Aflatoxin as it was one of the vital organs in addition to its innate function as a blood filter^[22].

The major blood supply for the kidney was directed to the renal cortex, so Aflatoxins were highly concentrated in the cortex rather than in the medulla^[23].

The animals received dose of aflatoxin 50 µg/kg by oral route according to Al-Ghasham *et al.*^[10]. The oral toxicity of Aflatoxin was of a particular concern to ensure public and consumer health^[24].

In our study, there was severe disruption of the renal cortex in AFB1-treated group, which was observed in the renal tubules and renal corpuscles. Most glomeruli were degenerated, others were segmented and others showed intraglomerular congestion. Some renal corpuscles showed widening of the urinary spaces; this is in agreement with Abdel-Hamid and Firgany^[25].

The epithelial cells lining renal tubules were highly active ion transporting cells and have electro-charged surfaces, thus they were very susceptible to toxic injury, as they absorbed and concentrated toxins^[24].

Our results showed chromatolysis of most of the nuclei of renal tubular cells of AFB1 treated groups. The nuclei were either large or small & some of the affected nuclei were expelled in the tubular lumen, this was in accordance with other researchers^[24].

The nuclear changes detected in our study could be explained by the effect of a high electrophilic metabolic product of AFB1 metabolism causing inhibition of mRNA, DNA-dependent RNA polymerase and subsequently protein synthesis. This compound forms covalent bonds with nucleophilic sites of macromolecules such as DNA, RNA, and proteins.^[26]

The renal tubular cells of AFB1 treated groups showed also vacuolar degeneration, sloughing of some epithelial

cells and intratubular epithelial debris. These results also were recorded by Bilgic and Yesildere^[27].

The generation of a reactive metabolite, namely AFB1-8,9-epoxide was the cause of the renal toxicity of AFB1. AFB1-8,9-epoxide reacted with DNA to yield the 8,9-dihydro-8-(N7-guanyl)-9-hydroxyaflatoxin B1 adduct (AFB1-N7-Gua), which had been positively correlated with DNA strand breaks. This adduct had also been shown to be positively correlated with the development of renal lesions^[28]. Meki *et al.*^[21] added that AFS produce apoptosis.

Significant increase in lipid peroxidation (LPO) was produced by AFB1 administration. Production of free radicals and decreased antioxidant status resulted in increased lipid peroxides. It had been linked to altered membrane structure and enzyme inactivation^[29].

Congestion of renal blood vessels and interstitial infiltration with mononuclear cells detected in AFB1 group in our study were also recorded by Mohamed and Mohamed^[30]. The release of endothelial relaxation factor nitric oxide (NO) caused by the direct effect of AFs on the endothelial cells of the blood vessels is the cause of congestion and dilatation of the blood vessels^[31].

The production of free radicals that triggered inflammation caused induction of cytokines and enhanced leukocyte trafficking and this result in the interstitial cellular infiltration in the AFB1 group as explained by Soliman and Tawfik^[32].

By Mallory stain, AFB1 group showed increased collagen deposition. These findings were supported by study done by Abdel-Hamid and Firgany^[25] who added that AFB1 causes focal fibrosis and degeneration.

The histochemical results were found to be parallel with histological findings. PAS reaction in AFB1 treated group showed weak PAS reaction in Bowman's capsule and brush borders of some renal tubules. This could be confirmed by a study on the liver rats given AFB1 showed focal glycogen loss^[33]. In other research done by El- Sayed *et al.*^[34] who explained that by the loss in capacity of the cells to metabolize the glycogen or might be attributed to the disturbed role of Golgi apparatus in polysaccharides synthesis.

Electron microscopic results of AFB1 group showed enlarged fused foot processes of the podocytes and fused endothelial cells. A previous study carried out by Abdel-Hamid and Firgany^[25] who has displayed similar glomerular affection.

EM results of AFB1 also showed that, some epithelial cells lining the tubules revealed cytoplasmic vacuolations and abnormal mitochondria. These results were recorded by

Martinez-de-Anda *et al.*^[35]. Fungal metabolites could alter the mitochondrial structure through its inhibitory effect on protein and enzyme biosynthesis as mentioned by Payne and Brown who performed genetic studies on aflatoxin biosynthesis in *Aspergillus flavus* and *A. parasiticus*, and sterigmatocystin biosynthesis in *A. nidulans*, led to the cloning of 17 genes responsible for 12 enzymatic conversions in the AF/ST pathways. Vacuolations of the cytoplasm of cells of the tubules had been demonstrated to be due to potassium depletion that is a feature of the diuretic stage of acute tubular necrosis^[37].

In normal kidney, PAX2 nuclear staining was seen in distal convoluted tubules, thick Henle loops, and collecting duct^[38]. PAX2 expression is not detected in mature glomeruli and proximal tubule^[39].

Some investigations found that PAX2 took part in the pathogenesis of glomerulosclerosis^[40] which showed dysregulation of shape of podocyte in idiopathic collapsing glomerulopathy, and renal cell carcinoma^[41].

In our study, PAX2 reaction showed increased expression in the podocytes of Aflatoxin treated group. This was in agreement with the previous researches^[42]. Also, another study performed by Ohtaka *et al.*^[43] found that the abnormal expression of PAX2 in podocytes might have an important role in the initiation of glomerular injury.

In glomerulosclerosis there was thickening of the glomerular basement membrane and deposition of collagen were also observed in the tubulointerstitium where inflammatory infiltrates were prominent^[44] and these findings were observed in our study.

This could be explained by the up regulation of the PAX2 gene expression induced by reactive oxygen species (ROS) which also can mediate PAX2 gene expression^[45].

The statistical results showed significant changes in body and kidney weights of all studied groups as compared to control group, this could be explained by the short period of our study (14 days). Similar results were observed by a previous researchers Abdel-Hamid and Firgany^[25].

There were increased concentrations of serum creatinine and urea in AFB1 group. These results were in agreement with the findings of Al-Ghasham *et al.*^[10], who reported that the creatinine and urea in AFB1 treated group were significantly higher than in the control group, but contraindicated with another findings of Abdel-Hamid and Firgany^[25] who reported that the serum creatinine and urea showed non-significant increase in AFB1 treated group.

The increase of serum urea and creatinine matched with kidney damage could be explained by the disturbed transportation function of epithelial cells in collecting

tubules and diffuse impairment of proximal tubules function as has been previously reported by Umar *et al.*^[46].

Persistent histological changes were observed in subgroup IIIb. Moderate affection of the structure of the renal cortex was observed. The normal appearing renal corpuscles were not recovered to the control group picture. The renal tubules were moderately affected compared with the AFB1 treated group, some of their cells showed cytoplasmic vacuolations with darkly stained nuclei. Bowman's capsule and renal tubules showed moderate amount of collagenous fibers, minimal PAS reaction and moderate expression of PAX2. The recovery subgroup (subgroup IIIb) showed highly significant increase in mean of serum urea and creatinine levels compared to control group. Our results were in agreement with previous study done by Omar^[47] who proved that the recovery subgroup showed partial improvement.

However, co-administration of dates with aflatoxin showed partial protection of the kidney against the hazardous effects of aflatoxin. Dates were given in a dose of 10 mg/kg according to Al-Ghasham *et al.*^[10].

Mild affection of the structure of the renal cortex was observed in group IV by H& E stain. Nearly normal appearing renal corpuscles were surrounded by the nearly intact renal tubules similar to that of the control. Almost all their cells of the renal tubules were mildly affected compared with the AFB1 treated group and had vesicular nuclei. Mild cellular infiltration in the interstitium was observed. Bowman's capsule and renal tubules showed mild amount of collagenous fibers by M.T. stain, moderate PAS reaction and mild expression of PAX2 in podocytes.

As giving dates concomitantly with aflatoxin, it would protect the renal cortex of rats. This ameliorative effect of dates on the toxic effect of aflatoxin B1 on the rat kidney might be attributed to its antioxidant activity and the presence of compounds with potent free-radical-scavenging activity^[10].

In our study, serum urea and creatinine showed a statistical decrease in group IV than Aflatoxin treated group as compared to control group. The mechanism by which dates induce its protective activity is not clear, but Al-Ghasham *et al.*^[10] reported that date fruit has antioxidant and antimutagenic activity and this implicated the presence of compounds with potent free-radical-scavenging activity.

The present biochemical results were according to the findings of Al-Ghasham *et al.*^[10] who reported that creatinine and urea significantly lowered in AFB1 and dates treated group than the AFB1 treated group.

CONCLUSION

In conclusion, our study showed that aflatoxin B1 had marked toxic effects on the rat kidney. These effects were partially improved after cessation of treatment. On the other hand co-administration of dates with aflatoxin B1 showed amelioration of structural and biochemical kidney affection and caused better protection than that detected in the recovery subgroup.

CONFLICT OF INTEREST

There are no conflicts of interest.

REFERENCES

1. **McKean C.; Tang L.; Tang M.; Billam M.; Wang Z. and Theodorakis C.W. (2006):** "Comparative acute and combinative toxicity of aflatoxin B1 and fumonisin B1 in animals and human cells". *Food Chem Toxicol*; 44:868–876.
2. **Hussain I.; Anwar J.; Asi M.R.; Munawar M.A. and Kashif M. (2010):** "Aflatoxin M1 contamination in milk from five dairy species in Pakistan". *Food Control* 21(2): 122-124.
3. **Marin S.; Ramos A.J.; Cano-Sancho G. and Sanchis V. (2013):** "Mycotoxins: occurrence, toxicology, and exposure assessment". *Food Chem Toxicol*. 60:218–37.
4. **Strosnider H.; Azziz-Baumgartner E.; Banziger M.; Bhat R.V.; Breiman R. and Brune M.N. (2006):** "Workgroup report: public health strategies for reducing aflatoxin exposure in developing countries". *Environ Health Perspect*;114:1898–1903.
5. **Stoev S.D. (2015):** "Foodborne mycotoxicosis risk assessment and underestimated hazard of masked mycotoxins and joint mycotoxin effects or interaction". *Environ Toxicol Pharmacol*; 39:794–809.
6. **Liao S.; Shi D.; Clemons-Chevis C.L.; Guo S.; Su R. and Qiang P. (2014):** "Protective role of selenium on aflatoxin b1-induced hepatic dysfunction and apoptosis of liver in ducklings". *Biol Trace Elem Res*;162:296–301.
7. **Ekor M. (2013):** "The growing use of herbal medicines: issues relating to adverse reactions and challenges in monitoring safety". *Front Pharmacol*. 4: 177.
8. **Al-Shwyeh HA (2019):** "Date Palm (Phoenix dactylifera L.) Fruit as Potential Antioxidant and Antimicrobial Agents". *J Pharm Bioallied Sci*. 11(1): 1–11.
9. **Rahmani A.H.; Aly S.M.; Ali H.; Babiker A.Y.; Srikar S. and Khan A.A. (2014):** "Therapeutic effects of date fruits (Phoenix dactylifera) in the prevention of diseases via modulation of anti-inflammatory, anti-oxidant and anti-tumour activity". *Int J Clin Exp Med*. 7(3): 483–491.
10. **Al-Ghasham, A.; Ata H.S.; El-Deep S.; Meki A.R. and Shehada S. (2008):** "Study of protective effect of date and Nigella sativa on aflatoxin B1 toxicity". *International journal of health sciences*, 2(2): .26-44. PMID:21475486.
11. **Keiding R.; Horder M. and Gerhardt W. (1974):** "Recommended methods for the determination of four enzymes in blood". *Scand J Clin Lab Investig*. 33:291–306.
12. **Kiernan J. A. (2015):** "Histological and histochemical methods: Theory and practice 5th edition". Banbury, UK: Scion Publishing.
13. **Kuo J. (2007):** "Electron Microscopy: Methods and Protocols". *Methods in molecular biology* 369. Published by Springer Science & Business Media.
14. **Bancroft J.D. & Layton C.(2015):** "Bancroft's theory and practice of histological techniques". Elsevier Health Sciences.
15. **Li Li; Wu Y. & Zhang W. (2010):** "PAX2 re-expression in renal tubular epithelial cells and correlation with renal interstitial fibrosis of rats with obstructive nephropathy, Renal Failure". *Journal homepage, ISSN: 0886-022X*. 32:5, 603-611.

16. **Peat j. and Barton B. (2005):** "Medical Statistics: A Guide to Data Analysis and Critical Appraisal", First edition. Jennifer Peat, Hospital Statistician, The Children's Hospital at Westmead, Australia. Belinda Barton, The Children's Hospital.
17. **AOAC (2007):** Association of Official Analytical Chemists. Official methods of analysis of A.O.A.C. International 17th Ed., Nature Toxins, Arlington, Virginia, USA, chapter 49.
18. **AOAC (2000):** Official methods of analysis of the Association of Analytical Chemists. Edited by H. William, 17th Ed., Vol II, Association of Official Analytical Chemists, Arlington VA.
19. **Abdel-Sattar W.M.; Sadek K.M.; Elbestawy A.R. and Mourad D.M. (2019):** "The Protective Role of Date Palm (Phoenix Dactylifera Seeds) against Aflatoxicosis in Broiler Chickens Regarding Carcass Characteristics, Hepatic and Renal Biochemical Function Tests and Histopathology". *World's Veterinary Journal.* 9(2): 59-69.
20. **Souza M.F.; Tome A.R. and Rao V.S. (1999):** "Inhibition by the bioflavonoid termination of aflatoxin B1-induced lipid peroxidation in rat liver". *J Pharm Pharmacol.* 51:125–129.
21. **Meki A.R.; Esmail Eel-D.; Hussein A.A. and Hassanein H.M. (2004):** "Caspase-3 and heat shock protein-70 in rat liver treated with aflatoxin B1: effect of melatonin". *Toxicol.* 43(1):93-100.
22. **Choi C.H.J.; Zuckerman J.E.; Webster P. and Davis M.E. (2011):** "Targeting kidney mesangium by nanoparticles of defined size". *Proc Natl Acad Sci U S A.* 108(16): 6656–6661.
23. **Abdelhalim M.A.K. and Jarrar B.M. (2011):** "The appearance of renal cells cytoplasmic degeneration and nuclear destruction might be an indication of GNPs toxicity". *Lipids in Health and Disease.* 10: 147.
24. **Kamel E.S. (2012):** "Histological study on the effect of aflatoxin B1 on the renal tubules of adult rats". *The Egyptian Journal of Histology.* 36:246-252.
25. **Abdel-Hamid A.A.M. and Firgany A.L. (2015):** "Vitamin E supplementation ameliorates aflatoxin B1-induced nephrotoxicity in rats". *Acta Histochemica.* 117: 767–779.
26. **Heidtmann-Bermvenuti R.; Mendes G.L.; Scaglioni P.T; Badiale-Furlong E. and Souza-Soares L.A. (2011):** "Biochemistry and metabolism of mycotoxins, a review". *Afr J Food Sci.* 5:881–889.
27. **Bilgic H.N. and Yesildere T. (1992):** "kidney lesions in experimental aflatoxicosis in chicks. *Istanbul Univ Vet Fak Derg.* 18: 102-8.
28. **Chou M.W.; Chen W.; Mikhailova M.V.; Nichols J.; Weis C.; Jackson C.D.; Hart R.W.; and Chung K.T. (1997):** "Dietary restriction modulated carcinogen-DNA adduct formation and the carcinogen-induced DNA strand breaks". *Toxicol Lett.* 92:21–30.
29. **Niki E.; Yoshida Y.; Saito Y. and Noguchi N. (2005):** "Lipid peroxidation: mechanisms, inhibition and biological effects. *Biochem Biophys Res Commun.* 338:668–676.
30. **Mohamed M.A. and Mohamed M.H. (2009):** "Hemato-biochemical and pathological studies on aflatoxicosis and treatment of broiler chicks in Egypt". *Veterinaria Italiana,* 45 (2): 323–337. PMID: 20391383.
31. **Wang P.; Verin A.D.; Birukova A.; Gilbert McClain L.I.; Jacobs K. and Garcia J.G.N.(2001):** "Mechanisms of sodium fluoride-induced endothelial cell barrier dysfunction: role of MLC phosphorylation". *Am J Physiol Lung Cell Mol Physiol.* 281:L1472–L1483.
32. **Soliman G.M. and Tawfik S.M (2014):** "Histological and immunohistochemical study on the effect of aflatoxin B1 on the left ventricular muscle of adult male rabbit with reference to the protective role of melatonin". *The Egyptian Journal of Histology.* 37:655-666.
33. **Kanaoka Y. and Boyce J.A. (2004):** "Cysteinylleukotrienes and their receptors:

- Cellular distribution and function in immune and inflammatory responses". *J Immunol.* 173: 1503-1510.
- 34. El- Sayed A.F.A.; Mahmoud B.L; Ali A.A.Z. and El- Mazar H.F. (2004):** Thesis "Histological Study On The Kidney Of Both Adult Golden Hamsters And Those Infected With *Schistosoma Haematobium* Under The Effect of Commiphora Molmol (Mirazid)". Page 78&79.
- 35. Martínez-de-Anda A.; Valdivia A.G.; Jaramillo-Juárez F.; Reyes J.L.; Ortiz R. and Quezada T. (2010):** "Effects of aflatoxin chronic intoxication in renal function of laying hens". *Poult Sci.* 89:1622–1628.
- 36. Payne G.A. and Brown M.P. (1998):** "Genetics and physiology of Aflatoxin biosynthesis". *Annu Rev Phytopathol.* 36:329–362.
- 37. Al-Habib M.F.M.; Jaffar A.A. and Abdul-Ameer H.H (2007):** "Aflatoxin B1-Induced Kidney Damage in Rats" . *J Fac Med Baghdad.* Vol. 49, No. 1.
- 38. Ozcan A.; Zhai J.; Hamilton C.; Shen S.S.; Ro Y.J.; Krishnan B. and Truong L.D. (2005):** "PAX-2 in the Diagnosis of Primary Renal Tumors. Immunohistochemical Comparison With Renal Cell Carcinoma Marker Antigen and Kidney-Specific Cadherin". *Am J Clin Pathol.* 131:393-404.
- 39. Eccles M.R.; Wallis L.J.; Fidler A.E.; Spurr N.K.; Goodfellow P. and Reeve A.E. (1992):** "Expression of the Pax-2 gene in human fetal kidney and Wilms' tumor". *Cell Growth Differ.* 3:279–289.
- 40. Yang Y.; Gubler M.C. and Beaufile H. (2002):** "Dysregulation of podocyte phenotype in idiopathic collapsing glomerulopathy and HIV-associated nephropathy". *Nephron.* 91: 416–423.
- 41. Hueber P.A.; Waters P.; Clark P.; Eccles M. and Goodyer P. (2006):** "PAX2 inactivation enhances cisplatin-induced apoptosis in renal carcinoma cells". *Kidney Int.* 69: 1139–1145.
- 42. Waters A.M.; Wu M.Y.; Onay T.; Scutaru J.; Liu J.; Lobe C.G.; Quaggin S.E. and Piscione T.D. (2008):** "Ectopic notch activation in developing podocytes causes glomerulosclerosis". *J Am Soc Nephrol.* 19: 1139–1157.
- 43. Ohtaka A.; Ootaka T.; Sato H. and Ito S. (2002):** "Phenotypic change of glomerular podocytes in primary focal segmental glomerulosclerosis: developmental paradigm?". *Nephrol Dial Transplant.* 17 Suppl 9: 11–15.
- 44. Maric C.; Sandberg K. and Laborde C.H. (2004):** "Glomerulosclerosis and Tubulointerstitial Fibrosis are Attenuated with 17 B-Estradiol in the Aging Dahl Salt Sensitive Rat". *J Am Soc Nephrol* 15: 1546–1556
- 45. Chen Y.W.; Liu F.; Tran S.; Zhu Y.; Hébert M.J.; Ingelfinger J.R. and Zhang S.L. (2006):** "Reactive oxygen species and nuclear factor-kappa B pathway mediate high glucose-induced Pax-2 gene expression in mouse embryonic mesenchymal epithelial cells and kidney explants". *Kidney Int.* 70: 1607–1615.
- 46. Umar S.; Arshad A.; Ahmad B. and Arshad M. (2012):** "Clinico biochemical and hematological changes in broilers induced by concurrent exposure to aflatoxin B1 and ochratoxin A". *Journal of Public Health and Biological Sciences,* 1: 79–85. DOI: 10.13140/2.1.2854.3681.
- 47. Omar N.A. (2012):** "Effect of Some Aflatoxins on A Lymphatic Organ (Spleen) of Male Albino Rats (Histopathological study)". *The Egyptian Journal of Hospital Medicine.* 48:357-367.

الملخص العربي

التأثيرات التحسينية للتمور على سمية الأفلاتوكسين ب ١ المستحثة على القشرة الكلوية لذكور الجرذان البيضاء البالغة

دراسة نسيجية وكيميائية مناعية و بيوكيميائية

مها السيد سليمان^١، ريم محمد غريب الشرقاوي^٢، منى محمد حسن سليمان^٢، غادة حسن الصيفي^٣، رانيا إبراهيم ياسين^٤

^{١,٢,٤,٥} قسم الأنسجة وبيولوجيا الخلية بكلية الطب جامعة المنوفية

^٣ باحث بقسم الأحياء الدقيقة والمناعة ، قسم البيطرة ، المركز القومي للبحوث ، الدقي ، مصر

المقدمة: يعتبر أفلاتوكسين ب ١ من السموم الفطرية الشديدة. تعتبر التمور نباتات علاجية عالية الترياق. **الهدف من البحث:** لذا أجرينا هذه الدراسة للتحقيق في الآثار النسيجية والكيميائية المستحثة للأفلاتوكسين ب ١ على الأنسجة القشرية الكلوية لذكور الجرذان البيضاء البالغة والدور المحسن المحتمل للتمور.

طرق البحث: قد أجرى هذا البحث علي ٦٠ من ذكور الجرذان البيضاء البالغة تم تقسيمها إلى أربع مجموعات رئيسية: المجموعة الضابطة (المجموعة الأولى) ، مجموعة التمور المعالجة (المجموعة الثانية) ، المجموعة المعالجة بالأفلاتوكسين ب ١ (المجموعة الثالثة) ، تمت التضحية بنصفهم بعد أسبوعين (المجموعة الفرعية IIIa) وترك النصف الآخر دون أي علاج لمدة أسبوعين آخرين كمجموعة فرعية للشفاء (المجموعة الفرعية IIIb) ومجموعة الأفلاتوكسين والتمور المعالجة (المجموعة الرابعة). في نهاية التجربة ، قمنا بتخدير الحيوانات وأخذنا عينات الدم من أجل وظائف الكلى ثم قمنا بتشريح الكليتين ومعالجتهما من أجل الدراسة النسيجية والكيميائية المناعية و البيوكيميائية.

النتائج: أظهرت الشرائح المصبوغة بصبغة الهيماتوكسلين و الايوسين من المجموعة الفرعية IIIa تغيرات تنكسية مختلفة في القشرة الكلوية ، جنباً الي جنب مع زيادة ترسب الكولاجين كما توضح باستخدام صبغة المالموري. كان هناك تفاعل مكثف PAS في كبسولة بومان والغشاء القاعدي للأنايب الكلوية. تم مطابقة النتائج الميكروسكوبية الإلكترونية مع النتائج الميكروسكوبية الضوئية. كما كشفت الصبغة المناعية الكيميائية عن مكثف صبغة PAX٢ في الخلايا من المجموعة الفرعية IIIa. أظهر فحص المجموعة التي تركت بدون علاج تحسن جزئي كما أظهر فحص المجموعة الرابعة استعادة القشرة الكلوية إلى التركيب النسيجي الطبيعي تقريبا.

الخلاصة: ونستخلص من هذه الدراسة أن الأفلاتوكسين ب ١ له تأثير ضار شديد على القشرة الكلوية. ترك الكلي بدون علاج يؤدي الي تحسن جزئي. من ناحية أخرى ، أظهر التناول المشترك للتمور مع الأفلاتوكسين ب ١ تحسناً في التركيب النسيجي والبيوكيميائي للكلية وتسبب في حماية أفضل من تلك التي تم اكتشافها في المجموعة الفرعية للشفاء.